

<https://helda.helsinki.fi>

New genetic signals for lung function highlight pathways and chronic obstructive pulmonary disease associations across multiple ancestries

Understanding Soc Sci Grp

2019-03

Understanding Soc Sci Grp 2019 , ' New genetic signals for lung function highlight pathways and chronic obstructive pulmonary disease associations across multiple ancestries ' , Nature Genetics , vol. 51 , no. 3 , pp. 481-+ . <https://doi.org/10.1038/s41588-018-0321-7>

<http://hdl.handle.net/10138/313328>

<https://doi.org/10.1038/s41588-018-0321-7>

unspecified

publishedVersion

Downloaded from Helda, University of Helsinki institutional repository.

This is an electronic reprint of the original article.

This reprint may differ from the original in pagination and typographic detail.

Please cite the original version.

New genetic signals for lung function highlight pathways and chronic obstructive pulmonary disease associations across multiple ancestries

Nick Shrine^{1,92}, Anna L. Guyatt^{1,92}, A. Mesut Erzurumluoglu^{1,92}, Victoria E. Jackson^{1,2,3}, Brian D. Hobbs^{4,5}, Carl A. Melbourne¹, Chiara Batini¹, Katherine A. Fawcett¹, Kijoung Song⁶, Phuwanat Sakornsakolpat^{4,7}, Xingnan Li⁸, Ruth Boxall^{9,10}, Nicola F. Reeve¹, Ma'en Obeidat¹¹, Jing Hua Zhao¹², Matthias Wielscher¹³, Understanding Society Scientific Group¹⁴, Stefan Weiss¹⁵, Katherine A. Kentistou^{16,17}, James P. Cook¹⁸, Benjamin B. Sun¹⁹, Jian Zhou²⁰, Jennie Hui^{21,22,23,24}, Stefan Karrasch^{25,26,27}, Medea Imboden^{28,29}, Sarah E Harris^{30,31}, Jonathan Marten³², Stefan Enroth³³, Shona M. Kerr³², Ida Surakka^{34,35}, Veronique Vitart³², Terho Lehtimäki³⁶, Richard J. Allen¹, Per S. Bakke³⁷, Terri H. Beaty³⁸, Eugene R. Bleeker⁸, Yohan Bossé^{39,40}, Corry-Anke Brandsma⁴¹, Zhengming Chen⁹, James D. Crapo^{42,43}, John Danesh^{19,44,45,46}, Dawn L. DeMeo^{4,5}, Frank Dudbridge¹, Ralf Ewert⁴⁷, Christian Gieger⁴⁸, Amund Gulsvik³⁷, Anna L. Hansell^{49,50,51}, Ke Hao⁵², Joshua D. Hoffman⁶, John E. Hokanson⁵³, Georg Homuth¹⁵, Peter K. Joshi¹⁶, Philippe Joubert^{40,54}, Claudia Langenberg⁵⁵, Xuan Li¹¹, Liming Li⁵⁶, Kuang Lin⁹, Lars Lind⁵⁷, Nicholas Locantore⁵⁸, Jian'an Luan⁵⁵, Anubha Mahajan⁵⁹, Joseph C. Maranville⁶⁰, Alison Murray⁶¹, David C. Nickle^{60,62}, Richard Packer¹, Margaret M. Parker⁴, Megan L. Paynton¹, David J. Porteous^{30,31}, Dmitry Prokopenko⁴, Dandi Qiao⁴, Rajesh Rawal^{48,63}, Heiko Runz⁶⁰, Ian Sayers⁶⁴, Don D Sin^{11,65}, Blair H Smith⁶⁶, María Soler Artigas^{67,68,69}, David Sparrow^{70,71}, Ruth Tal-Singer⁵⁸, Paul R. H. J. Timmers¹⁶, Maarten Van den Berge⁷², John C. Whittaker⁷³, Prescott G. Woodruff⁷⁴, Laura M. Yerges-Armstrong⁶, Olga G. Troyanskaya^{75,76}, Olli T. Raitakari^{77,78}, Mika Kähönen⁷⁹, Ozren Polašek^{16,80}, Ulf Gyllensten³³, Igor Rudan¹⁶, Ian J. Deary^{30,81}, Nicole M. Probst-Hensch^{28,29}, Holger Schulz^{25,27}, Alan L. James^{21,82,83}, James F. Wilson^{16,32}, Beate Stubbe⁴⁷, Eleftheria Zeggini^{84,85}, Marjo-Riitta Jarvelin^{13,86,87,88,89}, Nick Wareham⁵⁵, Edwin K. Silverman^{4,5}, Caroline Hayward³², Andrew P. Morris^{18,59}, Adam S. Butterworth^{19,46}, Robert A. Scott⁷³, Robin G. Walters⁹, Deborah A. Meyers⁸, Michael H. Cho^{4,5}, David P. Strachan⁹⁰, Ian P. Hall^{64,92}, Martin D. Tobin^{1,91,92*} and Louise V. Wain^{1,91,92*}

Reduced lung function predicts mortality and is key to the diagnosis of chronic obstructive pulmonary disease (COPD). In a genome-wide association study in 400,102 individuals of European ancestry, we define 279 lung function signals, 139 of which are new. In combination, these variants strongly predict COPD in independent populations. Furthermore, the combined effect of these variants showed generalizability across smokers and never smokers, and across ancestral groups. We highlight biological pathways, known and potential drug targets for COPD and, in phenome-wide association studies, autoimmune-related and other pleiotropic effects of lung function-associated variants. This new genetic evidence has potential to improve future preventive and therapeutic strategies for COPD.

Impaired lung function is predictive of mortality¹ and is the key diagnostic criterion for chronic obstructive pulmonary disease (COPD). Globally, COPD accounted for 2.9 million deaths in 2016 (ref. ²), and is one of the key causes of both years of life lost and

years lived with disability worldwide³. Determinants of maximally attained lung function and of lung function decline can influence the risk of developing COPD. Tobacco smoking is the single largest risk factor for COPD, although other environmental exposures

A full list of affiliations appears at the end of the paper.

and genetic makeup are important^{4,5}. Genetic variants associated with lung function and COPD susceptibility can provide etiological insights, assisting with risk prediction as well as drug target identification and validation⁶. Although there has been considerable progress in identifying genetic markers associated with lung function and risk of COPD^{4,7–19}, seeking a high yield of associated genetic variants is key to progressing knowledge because (1) implication of multiple molecules in each pathway will be needed to build an accurate picture of the pathways underpinning development of COPD; (2) not all proteins identified will be druggable and (3) combining information across multiple variants can improve prediction of disease susceptibility.

Through new detailed quality control and analyses of spirometric measures of lung function in the UK Biobank and expansion of the SpiroMeta Consortium, we undertook a large genome-wide association study (GWAS) of lung function. Our study entailed a near seven-fold increase in sample size over previous studies of similar ancestry to address the following aims: (1) to generate a high yield of genetic markers associated with lung function; (2) to confirm and fine-map previously reported lung function signals; (3) to investigate the putative causal genes and biological pathways through which lung function-associated variants act, and their wider pleiotropic effects on other traits; and (4) to generate a weighted genetic risk score for lung function and test its association with COPD susceptibility in individuals of European and other ancestries.

Results

Discovery of 139 new signals for lung function. We increased the sample size available for the study of quantitative measures of lung function in UK Biobank by refining the quality control of spirometry based on recommendations of the UK Biobank Outcomes Adjudication Working Group (Supplementary Note). Genome-wide association analyses of forced expired volume in 1 second (FEV₁), forced vital capacity (FVC) and FEV₁/FVC were undertaken in 321,047 individuals in UK Biobank (Supplementary Table 1) and in 79,055 individuals from the SpiroMeta Consortium (Supplementary Tables 2 and 3). A linear mixed model implemented in BOLT-LMM²⁰ was used for UK Biobank to account for relatedness and fine-scale population structure (Methods). A total of 19,819,130 autosomal variants imputed in both UK Biobank and SpiroMeta were analyzed. Peak expiratory flow (PEF) was also analyzed genome-wide in UK Biobank and up to 24,218 samples from SpiroMeta. GWAS results in UK Biobank were adjusted for the intercept of linkage disequilibrium (LD) score regression²¹, but SpiroMeta and the meta-analysis were not, as intercepts were close to 1.00 (Methods). All individuals included in the genome-wide analyses were of European ancestry (Supplementary Fig. 1 and Supplementary Note).

To maximize statistical power for discovery of new signals while maintaining stringent significance thresholds to minimize reporting of false positives, we adopted a study design incorporating both two-stage and one-stage approaches (Fig. 1). In the two-stage analysis, 99 new distinct signals, defined using conditional analyses²², were associated with one or more traits at $P < 5 \times 10^{-9}$ (ref. ²³) in UK Biobank and showed association ($P < 10^{-3}$) with a consistent direction of effect in SpiroMeta (tier 1 signals, Supplementary Fig. 2 and Supplementary Table 4). In the one-stage analysis, we meta-analyzed UK Biobank and SpiroMeta (up to 400,102 individuals), and identified 40 additional new distinct signals associated with one or more lung function traits reaching $P < 5 \times 10^{-9}$ (Supplementary Fig. 2 and Supplementary Table 4) that were also associated with $P < 10^{-3}$ separately in UK Biobank and in SpiroMeta, with consistent direction of effect (tier 2 signals). An additional 323 autosomal signals were significantly associated with one or more lung function traits in the meta-analysis of UK Biobank and SpiroMeta ($P < 5 \times 10^{-9}$) and reached $P < 10^{-3}$ for association in only one of

UK Biobank or SpiroMeta (tier 3 signals, Supplementary Table 5). Analysis of chromosome X variants in 359,226 individuals (321,027 UK Biobank and 38,199 SpiroMeta¹⁵) gave an additional five tier-3 signals. Only the 139 signals meeting tier-1 and tier-2 criteria were followed up. The strength and direction of association of the sentinel variant (the variant in each signal with the lowest P value) for these 139 new signals across all four lung function traits are shown in Fig. 2. Of the 139 signals, 131 were associated with at least two lung function traits at $P < 10^{-3}$, 8 signals were unique to FEV₁/FVC and no signals were unique to FEV₁, FVC or PEF at this threshold.

We assessed whether any of these 139 signals associated with lung function could be driven via an underlying association with smoking behavior (Methods). Only rs193686 (Supplementary Table 6) was associated with smoking behavior. Although rs193686 was associated with smoking initiation ($P = 9.18 \times 10^{-6}$), the allele associated with smoking initiation was associated with increased lung function in never smokers (FEV₁/FVC $P = 5.28 \times 10^{-10}$, Supplementary Table 7). Therefore, this signal was retained for further analysis.

A total of 279 signals of association for lung function. Of 157 previously published autosomal signals of association with lung function and COPD^{3,6–18}, 142 were associated at $P < 10^{-5}$ in UK Biobank (Methods, Supplementary Fig. 3 and Supplementary Table 8). Two sentinel variants (rs1689510 and rs11134789) were associated with smoking initiation (Supplementary Table 6), but were also associated with lung function in never smokers (Supplementary Table 7). SNP rs17486278 at *CHRNA5* and SNP rs11667314 near *CYP2A6* were both associated with cigarettes per day (Supplementary Table 6); neither was significantly associated with lung function among never smokers and so both were excluded from further analysis. This brings the total number of distinct signals of association with lung function to 279 (Supplementary Table 9). None of these variants showed interaction with ever-smoking status ($P > 1.8 \times 10^{-4}$, Methods and Supplementary Table 7). Using the effect estimates and allele frequencies and assuming a total heritability of 40% (refs. ^{24,25}; Methods), we calculated that the 140 previously reported lung function signals showing association in this study (UK Biobank $P < 10^{-5}$) explained 5.0%, 3.4%, 9.2% and 4.5% of the estimated heritability of FEV₁, FVC, FEV₁/FVC and PEF, respectively. The 139 new signals reported here explain an additional 4.3%, 3.3%, 3.9% and 3.3% of the estimated heritability, respectively.

Identification of putative causal genes. Bayesian refinement was undertaken for each signal, using the meta-analysis of UK Biobank and SpiroMeta, to identify the set of variants that were 99% probable to contain the underlying causal variant (assuming the causal variant has been analyzed; Methods, Supplementary Table 10 and Supplementary Data 1 and 2).

To identify putative causal genes for each signal, we identified deleterious variants and variants associated with gene expression (expression quantitative trait loci, eQTLs) or protein levels (protein quantitative trait loci, pQTLs) within each 99% credible set for all new and previously reported signals outside the human leukocyte antigen (HLA) region (where extensive linkage disequilibrium makes individual signals complex to define) (Methods).

There were 25 SNPs, located in 22 unique genes, that were annotated as potentially deleterious (Methods and Supplementary Table 11). Among our new signals, there were ten variants annotated as deleterious in nine different genes: *DOCK9* (rs117633128), *CEP72* (rs12522955), *BCHE* (rs1799807), *DST* (rs11756977), *KIAA0753* (rs2304977 and rs9889363), *LRRC45* (rs72861736), *BTC* (rs11938093), *MAB21L4* (rs6709469) and *IER5L* (rs184457). Of these, the missense variant in *BCHE* (rs1799807) had the highest posterior probability (0.996) in its respective credible set, was low in frequency (minor allele frequency = 1.95%) and leads to an

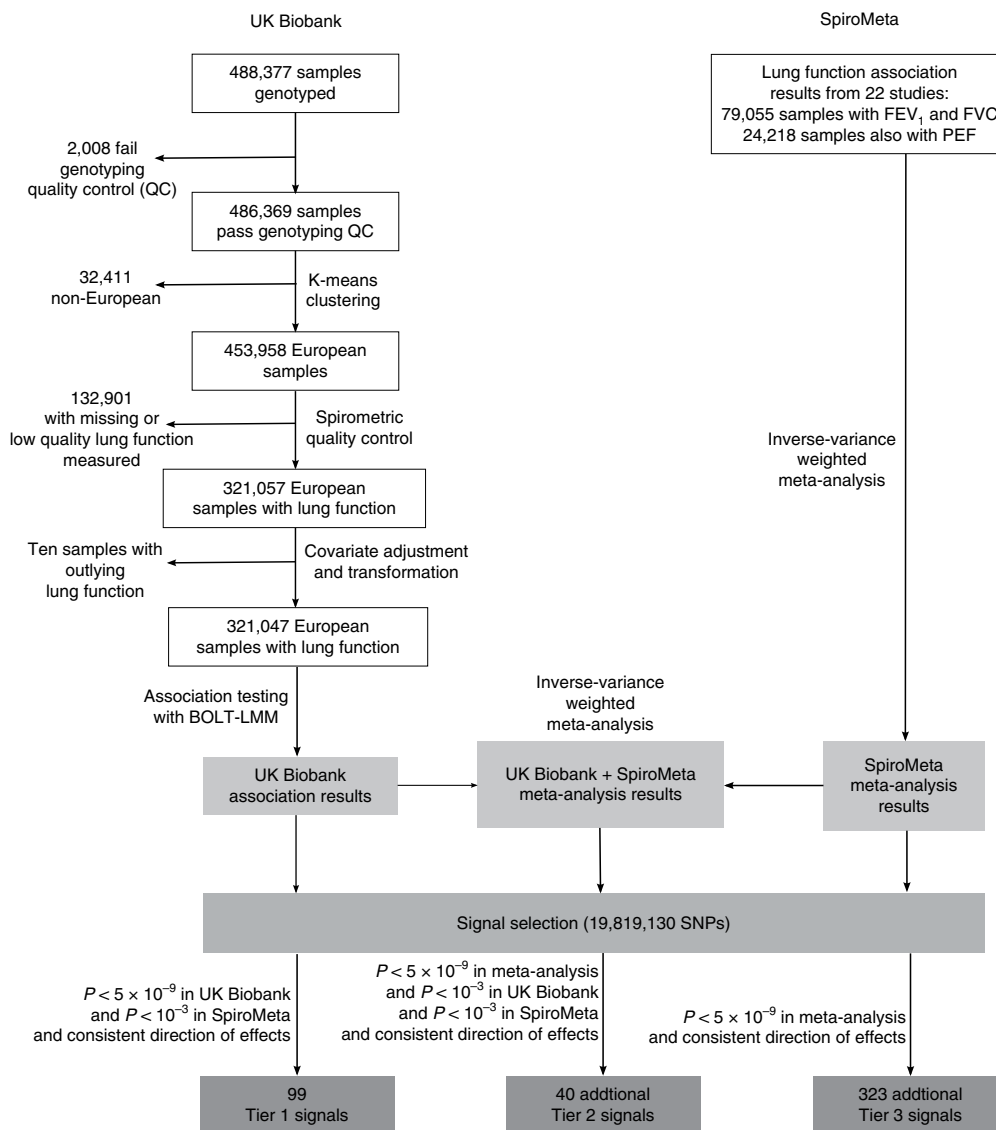


Fig. 1 | Study design. Tier 1 signals had $P < 5 \times 10^{-9}$ in UK Biobank and $P < 10^{-3}$ in SpiroMeta with consistent direction of effect. Tier 2 signals had $P < 5 \times 10^{-9}$ in the meta-analysis of UK Biobank and SpiroMeta with $P < 10^{-3}$ in UK Biobank and $P < 10^{-3}$ in SpiroMeta with consistent directions of effect. Signals with $P < 5 \times 10^{-9}$ in the meta-analysis of UK Biobank and SpiroMeta, and that had consistent directions of effect but did not meet $P < 10^{-3}$ in both cohorts, were reported as tier 3.

amino acid change from aspartic acid to glycine, which affects the function of the encoded butyrylcholinesterase enzyme by altering substrate binding²⁶. The two common missense variants in *KIAA0753* were within the credible set of new signal rs4796334. *KIAA0753*, *CEP72* and *LRRC45* all encode proteins with a role in ciliogenesis or cilia maintenance^{27–31}, and all are highly expressed in the airway epithelium³².

Variants in the 99% credible sets were queried in three eQTL resources to identify associations with gene expression in lung^{33–35} ($n = 1,111$; Supplementary Table 12), blood³⁶ ($n = 4,896$) and a subset of Genotype-Tissue Expression (GTEx)³⁷ tissues (maximum $n = 388$, Methods). The tissues included from GTEx were lung and blood, plus nine tissues containing smooth muscle (Methods). The latter were chosen based on previous reports of enrichment of lung function GWAS signals in smooth muscle-containing tissues^{18,38}. We identified 88 genes, implicated by 58 of the 279 signals, for which the most significant SNP associated with expression of that gene in the respective eQTL resource was within one of the 99% credible sets (Supplementary Table 13).

We checked credible set variants for association with protein levels in a pQTL study³⁹ comprising SNP associations for 3,600 plasma proteins (Methods). We found five proteins with a sentinel pQTL contained within our lung function credible set: ECM1, THBS4, NPNT, C1QTNF5 and SCARF2 (Supplementary Table 14).

In total, 107 putative causal genes were identified (Table 1), among which we highlight 75 for the first time as putative causal genes for lung function (43 implicated by a new signal and 32 newly implicated by a previous signal¹⁸).

Pathway analysis. We tested whether these 107 putative causal genes were enriched in gene sets and biological pathways (Methods), and found an enrichment of genes in elastic fiber and extracellular matrix organization pathways, and a number of gene ontologies including gene sets relating to the cytoskeleton and processes involved in ciliogenesis (Supplementary Table 15). Although the enrichment in elastic fiber-related pathways is consistent with our previous study¹⁸, enrichment in these pathways was further supported in this analysis by two new genes, *ITGAV* (at a new signal)

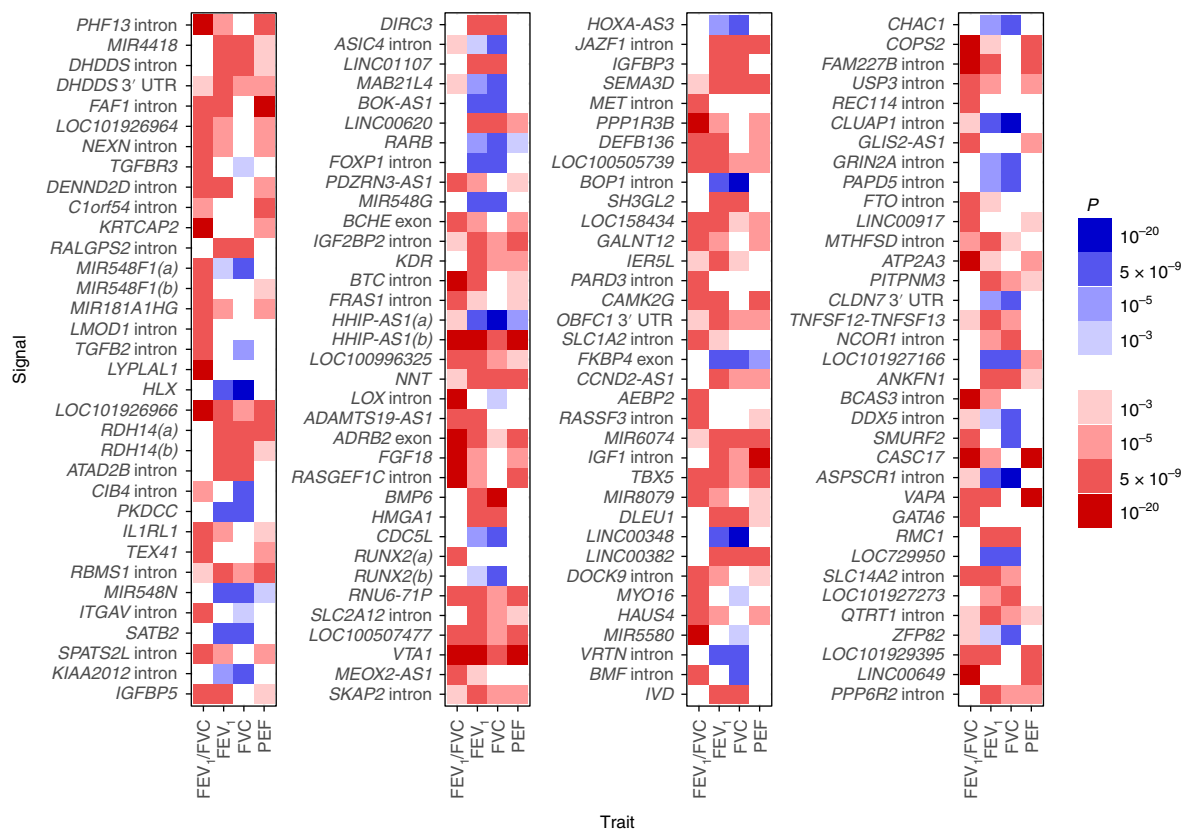


Fig. 2 | Strength and direction of association across four lung function traits for 139 novel signals. Signals are in chromosome and genomic position order from top to bottom then left to right. Red indicates a decrease in the lung function trait; blue indicates an increase. All effects are aligned to the allele associated with decreased FEV₁/FVC, hence the FEV₁/FVC column is only red or white. *P* values are from the meta-analysis of UK Biobank and SpiroMeta ($n=400,102$). The scale points are thresholds used for (1) confirmation in two-stage analysis and one-stage analysis ($P < 10^{-3}$); (2) confirmation of association of previous signals ($P < 10^{-5}$); (3) signal selection in two-stage and one-stage analysis ($P < 5 \times 10^{-9}$); capped at ($P < 10^{-20}$).

and *GDF5* (a newly implicated gene for a previously reported signal), and by strengthened eQTL evidence for *TGFB2* and *MFAP2* at two previously reported signals. The presence of *TGFB2*, *GDF5* and *SMAD3* in our list of 107 genes led to enrichment of a TGF- β superfamily signaling pathway (TGF-Core) and related gene ontology terms (Supplementary Table 15).

Functional enrichment analyses. Using stratified LD-score regression⁴⁰, we showed that FEV₁/FVC and FVC heritability are significantly enriched at variants overlapping histone marks that are specific to lung, fetal lung, and smooth muscle-containing cell lines. SNPs that overlap with H3K4me1 marks that are specific to fetal lung correspond to 6.99% of the input SNPs yet explain 57.09% ($P=2.85 \times 10^{-25}$) and 35.84% ($P=4.19 \times 10^{-21}$) of the SNP-chip heritability for FEV₁/FVC and FVC, respectively (Supplementary Table 16).

We also tested enrichment of (1) FEV₁/FVC and (2) FVC SNPs at DNase I hypersensitive site hotspots using GARFIELD⁴¹ (Methods). For FEV₁/FVC results, we saw significant enrichment across most cell lines with increased fold enrichment in fetal and adult lung, fetal muscle and fibroblasts (Supplementary Fig. 4a). For FVC, we saw similar broad significant enrichment without evidence of increased enrichment in a subset of tissues (Supplementary Fig. 4b), suggesting that SNPs influencing FVC may act via more complex and broader developmental pathways.

We used DeepSEA⁴² to identify whether our signals were predicted to have a chromatin effect in lung-related cell lines. We identified ten signals (including five new signals) for which the SNP with the largest posterior probability of being causal also had a

significant predicted effect on a DNase I hypersensitive site in lung-related cells (Supplementary Table 17). This included a new signal near *SMURF2* (rs11653958).

Drug targets. All 107 putative causal genes were investigated for known gene-drug interactions⁴³ (Supplementary Table 18). We highlight two examples of new genetic signals implicating targets for drugs in development for indications other than COPD. One of our new signals is an eQTL for *ITGAV*. *ITGAV* encodes a component of the $\alpha v \beta 6$ integrin heterodimer, which is inhibited by a monoclonal antibody in development for pulmonary fibrosis (NCT01371305) and for which the small molecule GSK3008348 (NCT03069989) is an antagonist⁴⁴. Integrins have an emerging role as local activators of TGF β and the $\alpha v \beta 6$ integrin heterodimer can activate latent TGF β ⁴⁵. In our study, the allele associated with reduced expression of *ITGAV* (Supplementary Table 13) was associated with increased lung function (Supplementary Table 9), suggesting that inhibitors of $\alpha v \beta 6$ integrin might also have a beneficial effect in COPD. Another new signal is associated with expression of *TNFSF13* (synonym *APRIL*), which encodes a cytokine of the TNF ligand family. Atacicept blocks B cell stimulation by TNFSF13 (as well as by BlyS) and reduced systemic lupus erythematosus disease activity in a recent phase 2b trial⁴⁶. In our study, the allele associated with decreased expression of *TNFSF13* was associated with reduced FEV₁, indicating that vigilance for pulmonary consequences of atacicept may be warranted.

Association with FEV₁/FVC and COPD in multiple ancestries. We constructed a genetic risk score (GRS) weighted by FEV₁/FVC effect

Table 1 | Genes implicated using gene expression data, protein level data and functional annotation

Gene	Phenotype	Other traits	Novel tier/ previous	Sentinel SNP	Position (b37)	COPD risk/alt	Functionally implicated genes
<i>DHDDS</i> (intron)	FVC	FEV ₁	Tier 2	rs9438626	1:26,775,367	G/C	<i>DHDDS</i> ^a
<i>DHDDS</i> (3'-UTR)	FEV ₁		Tier 1	rs12096239	1:26,796,922	C/G	<i>HMGN2</i> ^a , <i>DHDDS</i> ^a
<i>NEXN</i> (intron)	FEV ₁ /FVC		Tier 1	rs9661687	1:78,387,270	T/C	<i>NEXN</i> ^a
<i>DENND2D</i> (intron)	FEV ₁ /FVC	FEV ₁	Tier 1	rs9970286	1:111,737,398	G/A	<i>CEPT1</i> ^a , <i>CHI3L2</i> ^a , <i>DRAM2</i> ^a
<i>C1orf54</i> (intron)	PEF		Tier 1	rs11205354	1:150,249,101	C/A	<i>MRPS21</i> ^a , <i>RPRD2</i> ^a , <i>ECM1</i> ^b
<i>KRTCAP2</i>	FEV ₁ /FVC		Tier1	rs141942982	1:155153537	T/C	<i>THBS4</i> ^b
<i>RALGPS2</i> (intron)	FEV ₁	FVC	Tier 1	rs4651005	1:178,719,306	C/T	<i>ANGPTL1</i> ^a
<i>LMOD1</i> (intron)	FEV ₁ /FVC		Tier 2	rs4309038	1:201,884,647	G/C	<i>SHISA4</i> ^a
<i>ATAD2B</i> (intron)	FVC	FEV ₁	Tier 2	rs13009582	2:24,018,480	G/A	<i>UBXN2A</i> ^a
<i>PKDCC</i>	FVC	FEV ₁	Tier 1	rs4952564	2:42,243,850	A/G	<i>PKDCC</i> ^a
<i>ITGAV</i> (intron)	FEV ₁ /FVC		Tier 1	rs2084448	2:187,530,520	C/T	<i>ITGAV</i> ^a
<i>SPATS2L</i> (intron)	FEV ₁ /FVC		Tier 2	rs985256	2:201,208,692	C/A	<i>SPATS2L</i> ^a
<i>MAB21L4</i>	FVC		Tier 1	rs6437219	2:241,844,033	C/T	<i>MAB21L4</i> ^{a,c}
<i>MIR548G</i>	FVC	FEV ₁	Tier 1	rs1610265	3:99,420,192	T/C	<i>FILIP1L</i> ^a
<i>BCHE</i> (exon)	FEV ₁ /FVC		Tier 1	rs1799807	3:165,548,529	C/T	<i>BCHE</i> ^c
<i>BTC</i> (intron)	FEV ₁ /FVC	FEV ₁	Tier 1	rs62316310	4:75,676,529	G/A	<i>BTC</i> ^c
<i>LOC100996325</i>	FEV ₁	FEV ₁ /FVC	Tier 1	rs11739847	5:609,661	A/G	<i>CEP72</i> ^c
<i>RNU6-71P</i>	FEV ₁		Tier 1	rs2894837	6:56,336,406	G/A	<i>DST</i> ^e
<i>JAZF1</i> (intron)	FEV ₁	FVC, PEF	Tier 1	rs1513272	7:28,200,097	C/T	<i>JAZF1</i> ^a
<i>MET</i> (intron)	FEV ₁ /FVC		Tier 2	rs193686	7:116,431,427	T/C	<i>MET</i> ^b
<i>IER5L</i>	FEV ₁		Tier 2	rs967497	9:131,943,843	G/A	<i>CRAT</i> ^a , <i>PTPA</i> ^a , <i>IER5L</i> ^c
<i>DOCK9</i>	FEV ₁ /FVC		Tier 1	rs11620380	13:99,665,512	A/C	<i>DOCK9</i> ^c
<i>CHAC1</i>	FVC		Tier 1	rs4924525	15:41,255,396	A/C	<i>INO80</i> ^a , <i>CHP1</i> ^a , <i>RAD51</i> ^a
<i>ATP2A3</i>	FEV ₁ /FVC		Tier 1	rs8082036	17:3,882,613	G/C	<i>ATP2A3</i> ^a
<i>PITPNM3</i>	FEV ₁		Tier 2	rs4796334	17:6,469,793	A/G	<i>KIAA0753</i> ^{a,c} , <i>TXNDC17</i> ^a , <i>PITPNM3</i> ^a
<i>TNFSF12-TNFSF13</i>	FEV ₁		Tier 2	rs4968200	17:7,448,457	C/G	<i>TNFSF13</i> ^a , <i>SENP3</i> ^a
<i>NCOR1</i> (intron)	FVC		Tier 2	rs34351630	17:16,030,520	C/T	<i>ADORA2B</i> ^a , <i>TTC19</i> ^a
<i>ASPCR1</i> (intron)	FVC	FEV ₁	Tier 1	rs59606152	17:79,952,944	C/T	<i>LRRC45</i> ^c
<i>RMCI</i>	FVC	FEV ₁	Tier 1	rs303752	18:21,074,255	A/G	<i>RMCI</i> ^a
<i>ZFP82</i>	FVC		Tier 2	rs2967516	19:36,881,643	A/G	<i>ZFP14</i> ^a , <i>ZFP82</i> ^a
<i>MFAP2</i>	FEV ₁ /FVC	FVC, PEF	Previous	rs9435733	1:17,308,254	C/T	<i>MFAP2</i> ^a
<i>LOC101929516</i>	FEV ₁ /FVC	FEV ₁ , PEF	Previous	rs755249	1:39,995,074	T/C	<i>PABPC4</i> ^a
<i>TGFB2</i>	PEF		Previous	rs6604614	1:218,631,452	C/G	<i>TGFB2</i> ^a
<i>TRAF3IP1</i>	FEV ₁	FEV ₁ /FVC	Previous	rs6710301	2:239,441,308	C/A	<i>ASB1</i> ^c
<i>SLMAP</i> (intron)	FEV ₁	FVC, FEV ₁ /FVC, PEF	Previous	rs6445932	3:57,879,611	T/G	<i>SLMAP</i> ^a
<i>RSRC1</i> (intron)	FVC	FEV ₁	Previous	rs12634907	3:158,226,886	G/A	<i>RSRC1</i> ^a
<i>GSTCD</i> (intron)	FEV ₁	FVC, FEV ₁ /FVC	Previous	rs11722225	4:106,766,430	T/C	<i>INTS12</i> ^a
<i>NPNT</i> (intron)	FEV ₁ /FVC	FEV ₁ , FVC, PEF	Previous	rs34712979	4:106,819,053	A/G	<i>NPNT</i> ^{a,b}
<i>AP3B1</i> (intron)	FVC		Previous	rs425102	5:77,396,400	G/T	<i>AP3B1</i> ^a
<i>SPATA9</i>	FEV ₁ /FVC		Previous	rs987068	5:95,025,146	C/G	<i>RHOBTB3</i> ^a
<i>P4HA2-AS1</i>	FVC		Previous	rs3843503	5:131,466,629	A/T	<i>SLC22A5</i> ^a , <i>P4HA2</i> ^a , <i>C1QTNF5</i> ^b
<i>CYFIP2</i> (intron)	FEV ₁ /FVC	FEV ₁ , PEF	Previous	rs11134766	5:156,908,317	T/C	<i>ADAM19</i> ^a
<i>ADAM19</i> (intron)	FEV ₁ /FVC	FEV ₁ , PEF	Previous	rs11134789	5:156,944,199	A/C	<i>ADAM19</i> ^{a,c}
<i>DSP</i> (intron)	FEV ₁ /FVC		Previous	rs2076295	6:7,563,232	T/G	<i>DSP</i> ^a
<i>MIR588</i>	FVC	FEV ₁	Previous	rs6918725	6:126,990,392	T/G	<i>CENPW</i> ^a
<i>ADGRG6</i> (exon)	FEV ₁ /FVC	FVC, PEF	Previous	rs17280293	6:142,688,969	A/G	<i>ADGRG6</i> ^c
<i>C1GALT1</i> (intron)	FEV ₁ /FVC		Previous	rs4318980	7:7,256,490	A/G	<i>C1GALT1</i> ^a
<i>QSOX2</i> (3'-UTR)	FVC	FEV ₁	Previous	rs7024579	9:139,100,413	T/C	<i>QSOX2</i> ^a

Continued

Table 1 | Genes implicated using gene expression data, protein level data and functional annotation (Continued)

Gene	Phenotype	Other traits	Novel tier/ previous	Sentinel SNP	Position (b37)	COPD risk/alt	Functionally implicated genes
<i>DNLZ</i> (intron)	FVC		Previous	rs4073153	9:139,259,349	G/A	<i>SNAPC4^a, CARD9^a, INPP5E^a</i>
<i>CDC123</i> (intron)	FEV ₁ /FVC	FEV ₁ , FVC, PEF	Previous	rs7090277	10:12,278,021	T/A	<i>NUDT5^a</i>
<i>MYPN</i> (intron)	FVC	FEV ₁	Previous	rs10998018	10:69,962,954	A/G	<i>MYPN^c</i>
<i>EML3</i> (intron)	FEV ₁	FVC	Previous	rs71490394	11:62,370,155	G/A	<i>EEF1G^a, ROM1^{a,c}, EML3^{a,c}</i>
<i>ARHGEF17</i> (intron)	FEV ₁ /FVC	FEV ₁	Previous	rs2027761	11:73,036,179	C/T	<i>FAM168A^a, ARHGEF17^{a,c}</i>
<i>RAB5B</i> (intron)	FEV ₁		Previous	rs1689510	12:56,396,768	C/G	<i>CDK2^a</i>
<i>LRP1</i> (intron)	FEV ₁ /FVC	PEF	Previous	rs11172113	12:57,527,283	T/C	<i>LRP1^a</i>
<i>FGD6</i> (intron)	FEV ₁ /FVC		Previous	rs113745635	12:95,554,771	T/C	<i>FGD6^a</i>
<i>RPAP1</i>	FEV ₁ /FVC		Previous	rs2012453	15:41,840,238	G/A	<i>ITPKA^a, LTK^a, TYRO3^a, RPAP1^a</i>
<i>AAGAB</i>	FVC		Previous	rs12917612	15:67,491,274	A/C	<i>AAGAB^a, SMAD3^a, IQCH^a</i>
<i>THSD4</i> (intron)	FEV ₁ /FVC	FEV ₁ , PEF	Previous	rs1441358	15:71,612,514	G/T	<i>THSD4^a</i>
<i>IL27</i>	FEV ₁		Previous	rs12446589	16:28,870,962	A/G	<i>SBK1^a, TUFM^a, SGF29^a, SULT1A1^a, SULT1A2^{a,c}, SH2B1^a, NPIP87^a, CLN3^a, ATXN2L^a, EIF3C^a</i>
<i>MMP15</i> (intron)	FEV ₁ /FVC		Previous	rs11648508	16:58,063,513	G/T	<i>MMP15^a</i>
<i>SSH2</i> (intron)	FEV ₁ /FVC	PEF	Previous	rs2244592	17:28,072,327	A/G	<i>EFCAB5^a</i>
<i>FBXL20</i> (intron)	FVC	FEV ₁	Previous	rs8069451	17:37,504,933	C/T	<i>CDK12^a, FBXL20^a</i>
<i>MAPT-AS1</i>	FEV ₁	FVC, PEF	Previous	rs79412431	17:43,940,021	A/G	<i>LRRC37A4P^a, MAPT^a</i>
<i>TSEN54</i> (intron)	FEV ₁		Previous	rs9892893	17:73,525,670	G/T	<i>CASKIN2^a, TSEN54^c</i>
<i>LTBP4</i> (exon)	FEV ₁ /FVC	PEF	Previous	rs34093919	19:41,117,300	G/A	<i>LTBP4^c</i>
<i>ABHD12</i> (intron)	FEV ₁		Previous	rs2236180	20:25,282,608	C/T	<i>PYGB^{a,c}</i>
<i>UQC1</i> (5'-UTR)	FVC	FEV ₁ , PEF	Previous	rs143384	20:34,025,756	G/A	<i>UQC1^a, GDF5^a</i>
<i>SLC2A4RG</i> (intron)	FVC	FEV ₁	Previous	rs4809221	20:62,372,706	A/G	<i>LIME1^a</i>
<i>SCARF2</i> (intron)	FEV ₁	FEV ₁ , FVC	Previous	rs9610955	22:20,790,723	C/G	<i>SCARF2^{c,b}</i>

'Other traits' column lists the other lung function traits for which the sentinel was associated at $P < 5 \times 10^{-9}$ in the meta-analysis of UK Biobank and SpiroMeta. 'COPD risk/alt' column shows the COPD risk allele (i.e., FEV₁/FVC reducing) and the alternate ('alt') allele. In total, 107 putative causal genes were identified: 8 by both a deleterious variant and an eQTL signal (including *KIAA0753* implicated by two deleterious variants), 1 (*NPNT*) by both an eQTL and a pQTL signal, 1 (*SCARF2*) by both a deleterious variant and a pQTL signal, 13 by a deleterious variant only, 81 by an eQTL signal only and 3 by a pQTL signal only. ^aGenes implicated by eQTL signals: lung eQTL ($n = 1,111$) and blood eQTL ($n = 4,896$) data sets and 11 GTEx (V7) tissues were screened: artery aorta ($n = 267$), artery coronary ($n = 152$), artery tibial ($n = 388$), colon sigmoid ($n = 203$), colon transverse ($n = 246$), esophagus gastroesophageal junction ($n = 213$), esophagus muscularis ($n = 335$), lung ($n = 383$), small intestine terminal ileum ($n = 122$), stomach ($n = 237$) and whole blood ($n = 369$); see Supplementary Table 13 for direction of gene expression for the COPD risk (FEV₁/FVC reducing) allele. ^bGenes implicated by pQTL signals: pQTL look-up in 3,600 plasma proteins (n up to 3,300). ^cGenes implicated because they contain a deleterious variant (Supplementary Table 11).

sizes comprising all 279 sentinel variants, and tested for association with FEV₁/FVC and GOLD stage 2–4 COPD (FEV₁/FVC < 0.7 and FEV₁ < 80% predicted) in different ancestry groups in UK Biobank, and China Kadoorie Biobank (CKB) (Methods and Supplementary Table 19). UK Biobank participants of non-European ancestry were not included in the discovery analyses. The GRS was associated with a significant decrease in lung function and a corresponding significant increase in COPD risk in each of the independent ancestry groups (Fig. 3a).

We tested for a GRS interaction with smoking in individuals of European ancestry in UK Biobank⁴⁷. No statistical interaction was seen for FEV₁/FVC (interaction term −0.002 per s.d. change in GRS, 95% confidence interval (CI): [0.009, 0.005], $P = 0.532$), whereas the findings for COPD were consistent with a slightly smaller effect of the GRS in ever smokers (odds ratio (OR) for ever-smoking-GRS interaction term per s.d. change in GRS 0.96, 95% CI: [0.92, 0.99], $P = 0.015$).

The association of the GRS with COPD susceptibility was additionally tested in five independent COPD case-control studies (Supplementary Table 20 and Methods). Similar effect size estimates were seen across each of the five European ancestry studies (Fig. 3b); in the meta-analysis of these studies ($n = 6,979$ cases and 3,915 controls), the OR for COPD per s.d. of the weighted GRS was 1.55 (95% CI: [1.48, 1.62]), $P = 2.87 \times 10^{-75}$ (Supplementary Table 21). The GRS was also associated with COPD in individuals of

African-American ancestry in COPDGene ($P = 8.36 \times 10^{-7}$), albeit with a smaller effect size estimate, OR = 1.26 (95% CI: [1.15, 1.37]).

To aid clinical interpretation, we divided individuals in each of the five European-ancestry COPD case-control studies into deciles, according to their value of the weighted GRS. The OR for COPD in members of the highest GRS decile compared to the lowest GRS decile was 4.73 (95% CI: [3.79, 5.90]), $P = 3.00 \times 10^{-43}$ (Fig. 3c and Supplementary Table 22). We calculated the population-attributable risk fraction (Supplementary Note) and estimated that the proportion of COPD cases attributable to risk scores above the first GRS decile was 54.6% (95% CI: [50.6%, 58.4%]).

Incorporation of the GRS into a risk model already comprising available clinical information (age, sex, height and pack-years of smoking in COPDGene non-Hispanic whites) led to a statistically significant ($P = 3.33 \times 10^{-10}$) yet modest increase in the area under the curve, from 0.751 to 0.771 (Supplementary Note). Based on our estimated GRS relative risk and absolute risk estimates of COPD⁴⁸, we would expect the highest GRS-risk decile group of smokers to have an absolute risk of developing COPD by ~70 years of age of 82.4%, versus 17.4% for the lowest GRS decile (Supplementary Note).

Pleiotropy and phenome-wide association studies. As phenome-wide association studies (PheWASs) can provide evidence mimicking pharmacological interventions of drug targets in humans and informing drug development⁴⁹, we undertook a PheWAS of 2,411

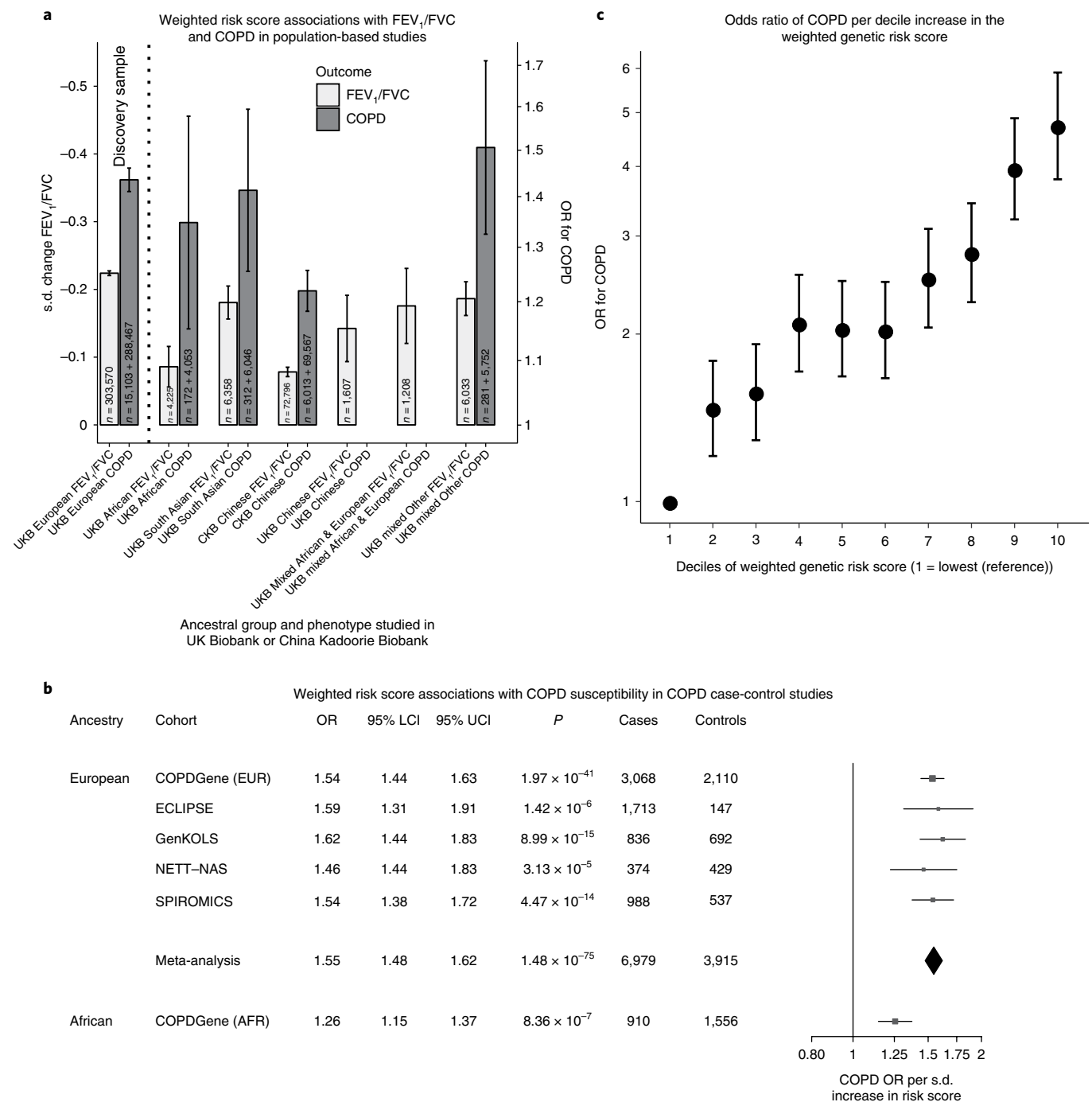


Fig. 3 | Association of weighted genetic risk score with COPD and FEV₁/FVC. **a**, Association of the weighted genetic risk score (wGRS) with FEV₁/FVC and COPD in UK Biobank (UKB) and CKB (Supplementary Table 19). Left-hand y-axis, s.d. change in FEV₁/FVC per s.d. increase in wGRS (light grey bars, n = total sample size). Right-hand y-axis, the translation of this effect to COPD (GOLD stage 2–4) OR per s.d. increase in wGRS in the same individuals for UKB ancestries with >100 COPD cases (dark grey bars, n = number of cases plus number of controls). Whiskers represent 95% CI. Some variants in the wGRS were discovered in UKB Europeans, therefore UKB Europeans are shown for reference only (far left, discovery sample). All other ancestral groups are independent to UKB Europeans. **b**, OR for COPD per s.d. increase in wGRS in six study groups. COPD was defined using GOLD 2–4 criteria (Supplementary Table 21: mean and s.d. of risk scores). The vertical black line indicates the null effect (OR = 1). The point estimate of each study is represented by a box proportional to study weight; whiskers represent 95% CI. The diamond represents a fixed-effect meta-analysis of the five European-ancestry groups, the width of which represents the 95% CI (I^2 statistic = 0). **c**, OR for COPD according to deciles of the wGRS, with decile 1 (the 10% of individuals with the lowest GRS) as the reference group. Each point represents a meta-analysis of results for a given comparison (for example, decile 2 versus reference, or decile 3 versus reference) in five external European-ancestry study groups (COPDGene, ECLIPSE, GenKOLS, SPIROMICS and NETT-NAS). Deciles were calculated and models were run in each group separately. Error bars show 95% CI (Supplementary Table 22).

phenotypes in UK Biobank (Methods, Fig. 4 and Supplementary Table 23); 226 of the 279 sentinel variants were associated (false discovery rate (FDR) < 1%) with one or more traits and diseases

(excluding quantitative lung function traits). Some 85 of the lung function signals were associated with standing height. To investigate whether the genetic association signals for lung function were

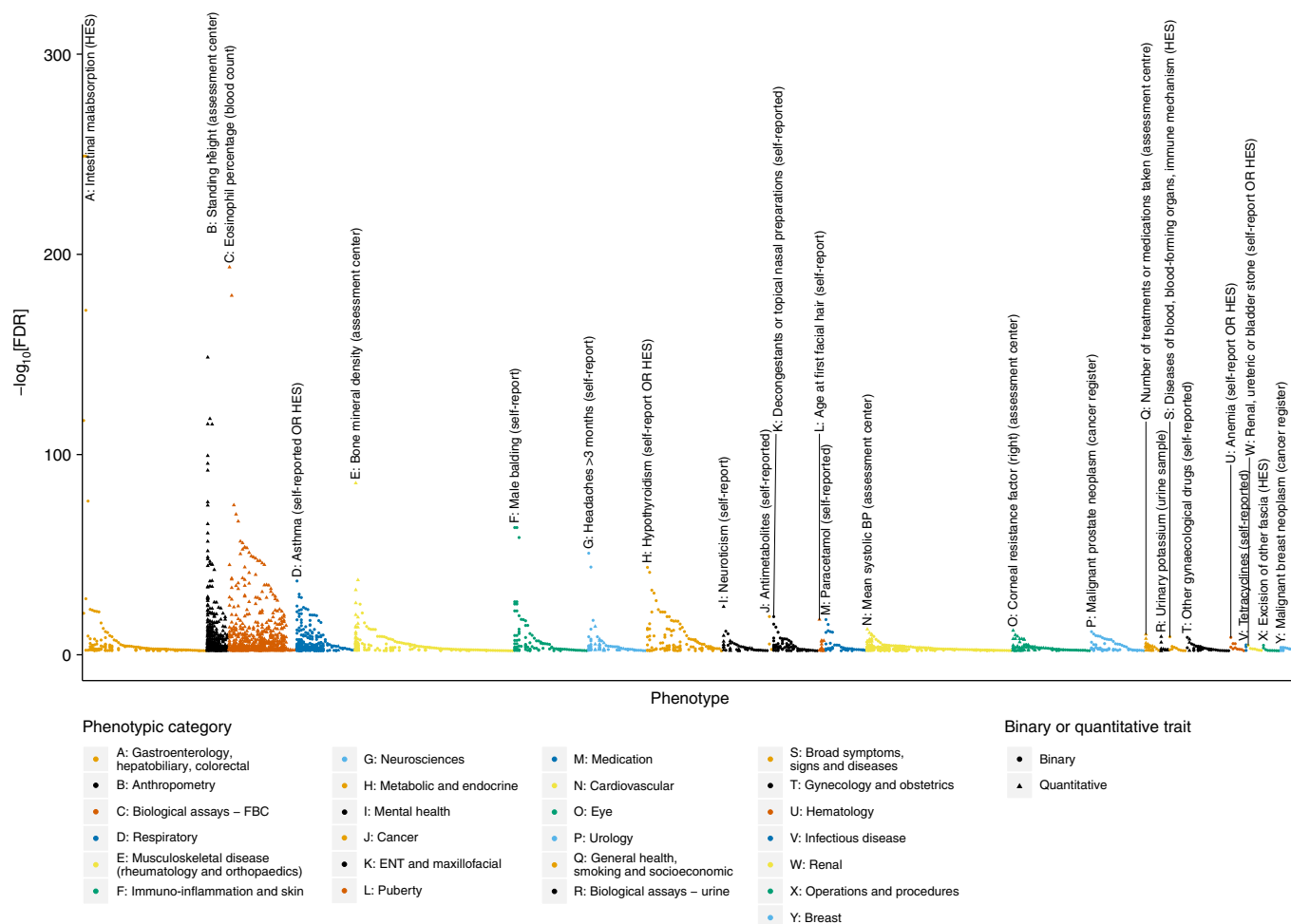


Fig. 4 | Individual PheWAS with 279 variants (traits passing FDR 1% threshold). Separate association of 279 variants with 2,411 traits (FDR < 1%) in UK Biobank (n up to 379,337). In each category, the trait with the strongest association, that is, highest $-\log_{10}[\text{FDR}]$, is shown first, followed by other traits in that category in descending order of $-\log_{10}[\text{FDR}]$. Categories are color coded, and outcomes are denoted with a circular or triangular point, according to whether they were coded as binary or quantitative. The top association per category is labeled with its rsID number, and a plain English label describing the trait. The letter at the beginning of each label allows easy cross-reference with the categories labeled in the legend. Zoomed-in versions of each category with visible trait names and directionality are available in Supplementary Fig. 10. These plots have signed $\log_{10}[\text{FDR}]$ values, where a positive values indicate that a positive SNP-trait association is concordant with the risk allele for reduced lung function (as measured by lower FEV_1/FVC). Tabulated results of all SNP-trait PheWAS associations associated at an FDR of < 1% are available in Supplementary Table 23.

driven by incomplete adjustment for height, we tested for correlation of effects on lung function in UK Biobank and height in a meta-analysis of UK Biobank and the GIANT consortium for 246 of the 279 signals that had a proxy variant in GIANT⁵⁰; there was no significant correlation (Supplementary Fig. 5). Additionally, the PheWAS identified associations with body composition measures such as fat-free mass (54 SNPs) and hip circumference (40 SNPs), as well as muscle strength (32 SNPs, grip strength). Some 114 of the 279 SNPs were associated with several quantitative measures of blood count, including eosinophil counts and percentages (25 SNPs). Twenty-five of our SNPs were also associated with asthma including 12 SNPs associated with both asthma and eosinophil measures (Supplementary Table 24). Eight of these SNPs were in LD ($r^2 > 0.1$) with a SNP reported for association with asthma in previously published GWASs. We compared our observed effect sizes with those estimated after exclusion of all self-reported asthma cases and observed similar estimates (Supplementary Fig. 6), suggesting that the lung function associations we report are not driven by asthma.

We examined the specificity of genetic associations, given the potential for this to predict specificity of drug target modification, and found that 53 of the 279 signals were associated only with lung function and COPD-related traits. In contrast, 3 of our 279 signals were associated with >100 traits across multiple categories—among these rs3844313, a known intergenic signal near *HLA-DQB1*, was associated with 163 traits, and also had the strongest signal in the PheWAS, which was for association with intestinal malabsorption and celiac disease.

In our 279-variant weighted GRS PheWAS analysis (Supplementary Table 25), we found association with respiratory traits including COPD, chronic bronchitis, emphysema, respiratory failure, corticosteroid use and both pediatric and adult-onset asthma (Fig. 5a). The GRS was also associated with nonrespiratory traits including celiac disease, an intestinal autoimmune disorder (Fig. 5b). These pleiotropic effects on risk of autoimmune diseases were further confirmed by analysis of previously reported GWASs (Methods and Supplementary Table 26), which showed overlapping single-variant associations with Crohn's disease, ulcerative colitis,

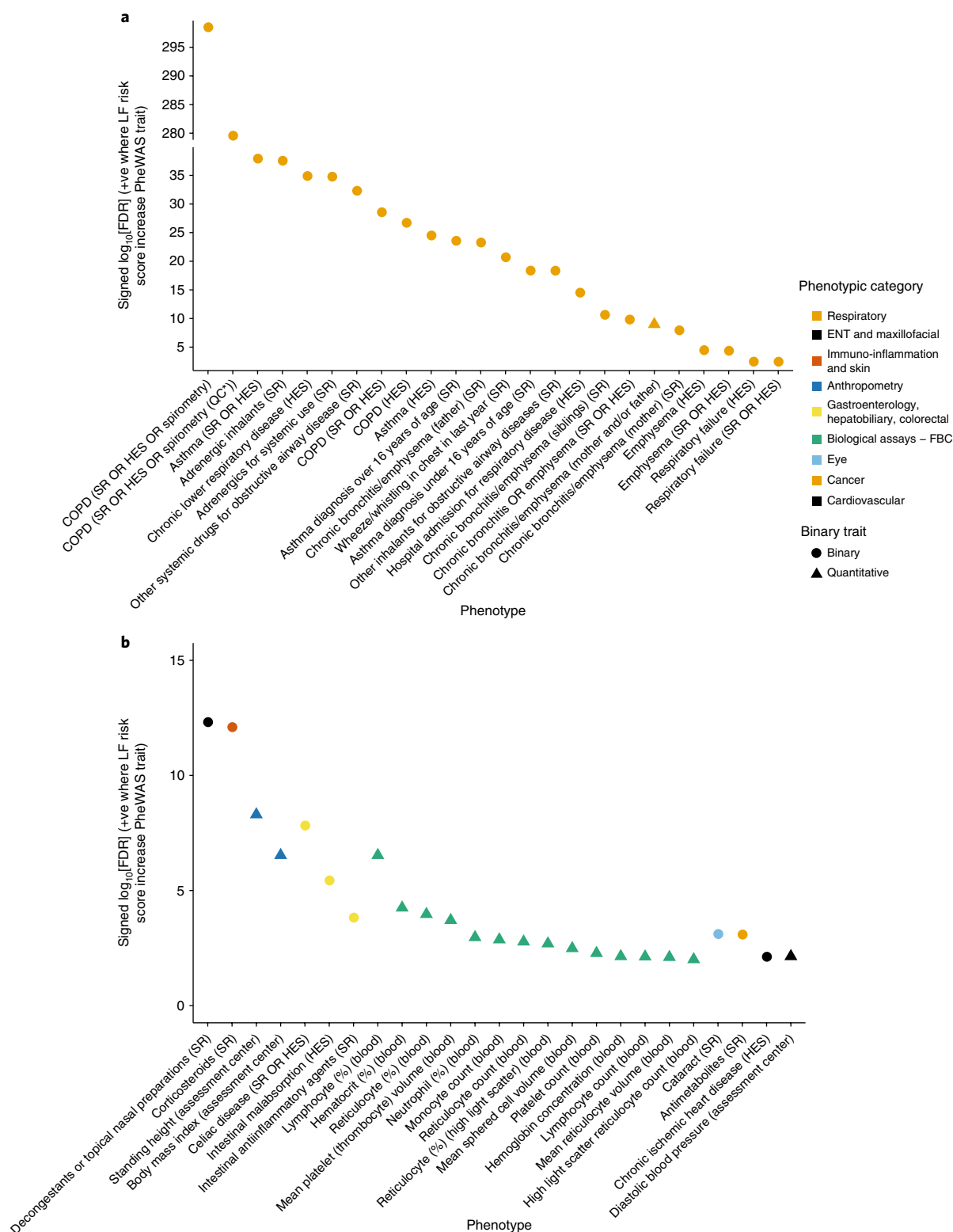


Fig. 5 | PheWAS with genetic risk score (traits passing FDR 1% threshold). Association of a 279 variant weighted genetic risk score with 2,453 traits (FDR < 1%) in UK Biobank (n up to 379,337). In each panel, the category with the strongest association, that is, highest $-\log_{10}[\text{FDR}]$, is shown first, followed by all other associations in that category, ordered by descending order of $-\log_{10}[\text{FDR}]$. Sample sizes varied across traits and are available in Supplementary Table 25, along with the full summary statistics for each association, plus details of categorization and plain English labels for each trait. Trait categories are color coded, and outcomes are denoted with a circular or triangular point, according to whether they were coded as binary or quantitative. The sign of the $\log_{10}[\text{FDR}]$ value is positive where an increase in the risk score (that is, greater risk of COPD, reduced lung function) is associated with a positive effect estimate for that trait. *QC refers to spirometry passing European Respiratory Society/American Thoracic Society criteria. SR, self-report; HES, hospital episode statistics. **a**, Associations with respiratory traits. **b**, Associations with all other traits. ENT, ear, nose and throat; FBC, full blood count.

psoriasis, systemic lupus erythematosus, IgA nephropathy, pediatric autoimmune disease and type 1 diabetes.

Discussion

The large sample size of our study, achieved by our refinement of the spirometry in UK Biobank and inclusion of the substantially expanded SpiroMeta consortium data set, has doubled the yield of lung function signals to 279. Fine-mapping of all new and previously reported signals, together with gene and protein expression analyses with improved tissue specificity and stringency, has implicated new genes and pathways, highlighting the importance of cilia development, TGF- β signaling via SMAD3, and elastic fibers in the etiology of airflow obstruction. Many of the genes and pathways reported here contain druggable targets; we highlight examples in which the genetic variants mimicking therapeutic modulation of targets may have opposing effects on lung function. We have developed and applied the first weighted GRS for lung function and tested it in independent COPD case-control studies. Our GRS shows stronger association and larger effect-size estimates than a previous GRS in European-ancestry populations¹⁸, as well as generalizability to other ancestry groups. We undertook the first comprehensive PheWAS for lung function signals, and report genetic variants with apparent specificity of effects and others with pleiotropic effects that might indicate shared biological pathways between different diseases.

For the first time in a GWAS of lung function, we report an enrichment of genes involved in ciliogenesis (including *KIAA0753*, *CDK2* and *CEP72*). Defects in primary cilia as a result of highly deleterious mutations in essential genes lead to ciliopathies known to affect multiple organ systems. We found an enrichment of genes with a role in centriolar replication and duplication, core processes in primary and motile cilia formation. Mutations in *KIAA0753* cause the ciliopathies Joubert syndrome and orofacioidigital syndrome²⁸. Reduced airway motile cilia function impacting mucus clearance is a feature of COPD, but it has not been clear whether this is causal or the consequence of damage by external factors such as smoking or infection. Our findings suggest that impaired ciliary function might be a driver of the disease process. We have previously shown enrichment of rare variants in cilia-related genes in heavy smokers without airflow obstruction⁵¹.

New signals implicating *ITGAV* and *GDF5*, as well as stronger support for *TGFB2* and *MFAP2* as probable causal genes, provide new genetic support for the importance of elastic fiber pathways in lung function and COPD¹⁸. The elastic fibers of the extracellular matrix are disrupted in COPD⁵². As the breakdown of elastic fibers by neutrophil elastase leads to emphysema in individuals with α_1 -antitrypsin deficiency, we also assessed the association with the *SERPINA1* Z allele, which was not associated with FEV₁/FVC in our study (rs28929474, $P=0.109$ in UK Biobank).

Smoking and genetic risk both have important effects on lung function and COPD. For lung function, we found no interaction between smoking and individual variants, and for FEV₁/FVC we found no interaction between smoking status and the weighted GRS. However, for COPD, a weak smoking-GRS interaction was observed. Although the weighted GRS showed a strong association with COPD susceptibility and a high attributable risk, we do not claim that this would represent an appropriate method of screening for COPD risk. Importantly, our findings demonstrate the high absolute risk among genetically susceptible smokers (82.4% by ~70 years of age).

We used two complementary study designs to maximize sample size for discovery and ensure robustness of findings by requiring independent support for association. Furthermore, through additional analysis of the spirometry data in UK Biobank and substantial expansion of the SpiroMeta consortium, we have markedly increased samples sizes to almost seven times those

included in previous studies. As no lower minor-allele-frequency threshold was applied in our analyses, an overall threshold of $P < 5 \times 10^{-9}$, as recommended for resequencing analyses of European-ancestry individuals²³, was applied. We identified the largest number of new signals in our more stringent two-stage design (tier 1, 99 new signals). Among the signals that we report as tier 3 (and did not include in further analyses), all reached $P < 10^{-3}$ in UK Biobank and 183 met a less stringent threshold of $P < 0.05$ in SpiroMeta.

Our study is the first to investigate genome-wide associations with PEF. PEF is determined by various physiological factors including lung volume, large airway caliber, elasticity of the lung and expiratory muscle strength, is used for monitoring asthma, and was incorporated in a recently evaluated clinical score for diagnosing COPD and predicting acute exacerbations of COPD⁵³. Overall, 133 of the 279 signals were also associated with PEF ($P < 10^{-5}$) and for 15 signals (including 4 new signals), PEF was the most significantly associated trait. Notably, a signal near *SLC26A9*, a known cystic fibrosis modifier gene⁵⁴, was highly significantly associated with PEF in UK Biobank ($P = 3.97 \times 10^{-66}$) and nominally significant in SpiroMeta ($P = 6.93 \times 10^{-3}$), with consistent direction of effect, but did not meet the tier 2 criteria. This could reflect the limited power for PEF in SpiroMeta (up to 24,218 for PEF compared to 79,055 for the other traits).

Examining associations of a given genetic variant with a wide range of human phenotypes is a valuable tool in therapeutic target validation. As in our PheWAS, it can highlight variants that show associations with one or more respiratory traits that might be expected to demonstrate greater target specificity than variants associated with many traits. Additionally, in some instances, association with multiple traits may indicate the relevance of drug repurposing. Association of a given SNP with multiple traits does not necessarily imply shared etiology, and further investigation is warranted. Our GRS PheWAS assesses broader genetic overlap between lung function and other traits and supports the evidence for some shared genetic determinants with autoimmune diseases.

In summary, our study has doubled the number of signals for lung function and provides new understanding and resources of utility for the development of therapeutics. The 279-variant GRS we constructed was associated with a 4.73-fold increased relative risk of moderate to severe COPD between highest and lowest deciles, such that we would expect >80% of smokers in the highest genetic-risk decile to develop COPD. The GRS was also predictive of COPD across multiple ancestral groups. Our PheWAS highlights both expected and unexpected associations relevant to respiratory and other systemic diseases. Investigating the nature of the pleiotropic effects of some of these variants will be of benefit for drug target identification and validation.

URLs. UK Biobank, <http://www.ukbiobank.ac.uk>; Ensembl, <https://www.ensembl.org/vep>; The Drug-Gene Interaction Database, <http://www.dgidb.org/downloads>; ChEMBL drug indications, <https://www.ebi.ac.uk/chembl/drug/indications>; EBI GWAS catalog, <https://www.ebi.ac.uk/gwas/>; GRASP catalog, <https://grasp.nhlbi.nih.gov/Overview.aspx>.

Online content

Any methods, additional references, Nature Research reporting summaries, source data, statements of data availability and associated accession codes are available at <https://doi.org/10.1038/s41588-018-0321-7>.

Received: 8 June 2018; Accepted: 27 November 2018;

Published online: 25 February 2019

References

- Young, R. P., Hopkins, R. & Eaton, T. E. Forced expiratory volume in one second: not just a lung function test but a marker of premature death from all causes. *Eur. Respir. J.* **30**, 616–622 (2007).
- GBD 2016 Causes of Death Collaborators. Global, regional, and national age-sex specific mortality for 264 causes of death, 1980–2016: a systematic analysis for the Global Burden of Disease Study 2016. *Lancet* **390**, 1151–1210 (2017).
- GBD 2016 Disease and Injury Incidence and Prevalence Collaborators. Global, regional, and national incidence, prevalence, and years lived with disability for 328 diseases and injuries for 195 countries, 1990–2016: a systematic analysis for the Global Burden of Disease Study 2016. *Lancet* **390**, 1211–1259 (2017).
- Hobbs, B. D. et al. Genetic loci associated with chronic obstructive pulmonary disease overlap with loci for lung function and pulmonary fibrosis. *Nat. Genet.* **49**, 426–432 (2017).
- Salvi, S. S. & Barnes, P. J. Chronic obstructive pulmonary disease in non-smokers. *Lancet* **374**, 733–743 (2009).
- Nelson, M. R. et al. The support of human genetic evidence for approved drug indications. *Nat. Genet.* **47**, 856–860 (2015).
- Wilk, J. B. et al. A genome-wide association study of pulmonary function measures in the Framingham Heart Study. *PLoS Genet.* **5**, e1000429 (2009).
- Repapi, E. et al. Genome-wide association study identifies five loci associated with lung function. *Nat. Genet.* **42**, 36–44 (2010).
- Hancock, D. B. et al. Meta-analyses of genome-wide association studies identify multiple loci associated with pulmonary function. *Nat. Genet.* **42**, 45–52 (2010).
- Soler Artigas, M. et al. Genome-wide association and large-scale follow up identifies 16 new loci influencing lung function. *Nat. Genet.* **43**, 1082–1090 (2011).
- Cho, M. H. et al. A genome-wide association study of COPD identifies a susceptibility locus on chromosome 19q13. *Hum. Mol. Genet.* **21**, 947–957 (2012).
- Loth, D. W. et al. Genome-wide association analysis identifies six new loci associated with forced vital capacity. *Nat. Genet.* **46**, 669–677 (2014).
- Wain, L. V. et al. Novel insights into the genetics of smoking behaviour, lung function, and chronic obstructive pulmonary disease (UK BiLEVE): a genetic association study in UK Biobank. *Lancet Respir. Med.* **3**, 769–781 (2015).
- Lutz, S. M. et al. A genome-wide association study identifies risk loci for spirometric measures among smokers of European and African ancestry. *BMC Genet.* **16**, 138 (2015).
- Soler Artigas, M. et al. Sixteen new lung function signals identified through 1000 Genomes Project reference panel imputation. *Nat. Commun.* **6**, 8658 (2015).
- Hobbs, B. D. et al. Exome array analysis identifies a common variant in IL27 associated with chronic obstructive pulmonary disease. *Am. J. Respir. Crit. Care Med.* **194**, 48–57 (2016).
- Jackson, V. et al. Meta-analysis of exome array data identifies six novel genetic loci for lung function [version 3; referees: 2 approved]. *Wellcome Open Res.* **3**, 4 (2018).
- Wain, L. V. et al. Genome-wide association analyses for lung function and chronic obstructive pulmonary disease identify new loci and potential druggable targets. *Nat. Genet.* **49**, 416–425 (2017).
- Wyss, A. B. et al. Multiethnic meta-analysis identifies new loci for pulmonary function. *Nat. Commun.* **9**, 2976 (2017).
- Loh, P. R. et al. Efficient Bayesian mixed-model analysis increases association power in large cohorts. *Nat. Genet.* **47**, 284–290 (2015).
- Bulik-Sullivan, B. K. et al. LD Score regression distinguishes confounding from polygenicity in genome-wide association studies. *Nat. Genet.* **47**, 291 (2015).
- Yang, J. et al. Conditional and joint multiple-SNP analysis of GWAS summary statistics identifies additional variants influencing complex traits. *Nat. Genet.* **44**, 369–375 (2012).
- Pulit, S. L., de With, S. A. & de Bakker, P. I. Resetting the bar: Statistical significance in whole-genome sequencing-based association studies of global populations. *Genet. Epidemiol.* **41**, 145–151 (2017).
- Palmer, L. J. et al. Familial aggregation and heritability of adult lung function: results from the Busselton Health Study. *Eur. Respir. J.* **17**, 696–702 (2001).
- Wilk, J. B. et al. Evidence for major genes influencing pulmonary function in the NHLBI family heart study. *Genet. Epidemiol.* **19**, 81–94 (2000).
- Benyamin, B. et al. GWAS of butyrylcholinesterase activity identifies four novel loci, independent effects within BCHE and secondary associations with metabolic risk factors. *Hum. Mol. Genet.* **20**, 4504–4514 (2011).
- Hammarsjö, A., Wang, Z., Vaz, R. & Taylan, F. Novel KIAA0753 mutations extend the phenotype of skeletal ciliopathies. *Sci. Rep.* **7**, 15585 (2017).
- Stephen, J. et al. Mutations in KIAA0753 cause Joubert syndrome associated with growth hormone deficiency. *Hum. Genet.* **136**, 399–408 (2017).
- Loukil, A., Tormanen, K. & Sütterlin, C. The daughter centriole controls ciliogenesis by regulating Neurl-4 localization at the centrosome. *J. Cell Biol.* **216**, 1287–1300 (2017).
- He, R. et al. LRRC45 is a centrosome linker component required for centrosome cohesion. *Cell Rep.* **4**, 1100–1107 (2013).
- Conkar, D. et al. The centriolar satellite protein CCDC66 interacts with CEP290 and functions in cilium formation and trafficking. *J. Cell Sci.* **130**, 1450–1462 (2017).
- Uhlén, M. et al. Tissue-based map of the human proteome. *Science* **347**, 1260419 (2015).
- Hao, K. et al. Lung eQTLs to help reveal the molecular underpinnings of asthma. *PLoS Genet.* **8**, e1003029 (2012).
- Lamontagne, M. et al. Refining susceptibility loci of chronic obstructive pulmonary disease with lung eQTLs. *PLoS One* **8**, e70220 (2013).
- Obeidat, M. et al. GSTCD and INTS12 regulation and expression in the human lung. *PLoS One* **8**, e74630 (2013).
- Westra, H. J. et al. Systematic identification of trans eQTLs as putative drivers of known disease associations. *Nat. Genet.* **45**, 1238–1243 (2013).
- GTEX Consortium. Human genomics. The Genotype-Tissue Expression (GTEx) pilot analysis: multitissue gene regulation in humans. *Science* **348**, 648–660 (2015).
- Kundaje, A. et al. Integrative analysis of 111 reference human epigenomes. *Nature* **518**, 317–330 (2015).
- Sun, B. B. et al. Genomic atlas of the human plasma proteome. *Nature* **558**, 73–79 (2018).
- Finucane, H. K. et al. Partitioning heritability by functional annotation using genome-wide association summary statistics. *Nat. Genet.* **47**, 1228–1235 (2015).
- Itchikova, V. et al. Discovery and refinement of genetic loci associated with cardiometabolic risk using dense imputation maps. *Nat. Genet.* **48**, 1303–1312 (2016).
- Zhou, J. & Troyanskaya, O. G. Predicting effects of noncoding variants with deep learning-based sequence model. *Nat. Meth.* **12**, 931–934 (2015).
- Cotto, K. C. et al. DGIdb 3.0: a redesign and expansion of the drug-gene interaction database. *Nucleic Acids Res.* **46**, D1068–D1073 (2017).
- Slack, R. et al. P112 discovery of a novel, high affinity, small molecule $\alpha\beta 6$ inhibitor for the treatment of idiopathic pulmonary fibrosis. *QJM* **109**, S60–S60 (2016).
- Raab-Westphal, S., Marshall, J. F. & Goodman, S. L. Integrins as therapeutic targets: successes and cancers. *Cancers (Basel)* **9**, e110 (2017).
- Merrill, J. T. et al. Efficacy and safety of atacicept in patients with systemic lupus erythematosus: results of a twenty-four-week, multicenter, randomized, double-blind, placebo-controlled, parallel-arm, phase IIb study. *Arthritis Rheumatol.* **70**, 266–276 (2018).
- Aschard, H. et al. Evidence for large-scale gene-by-smoking interaction effects on pulmonary function. *Int. J. Epidemiol.* **46**, 894–904 (2017).
- Lokke, A., Lange, P., Scharling, H., Fabricius, P. & Vestbo, J. Developing COPD: a 25 year follow up study of the general population. *Thorax* **61**, 935–939 (2006).
- Pulley, J. M. et al. Accelerating precision drug development and drug repurposing by leveraging human genetics. *Assay. Drug. Dev. Technol.* **15**, 113–119 (2017).
- Yengo, L. et al. Meta-analysis of genome-wide association studies for height and body mass index in ~700,000 individuals of European ancestry. *Hum. Mol. Genet.* **27**, 3641–3649 (2018).
- Wain, L. V. et al. Whole exome re-sequencing implicates CCDC38 and cilia structure and function in resistance to smoking related airflow obstruction. *PLoS Genet.* **10**, e1004314 (2014).
- Black, P. N. et al. Changes in elastic fibres in the small airways and alveoli in COPD. *Eur. Respir. J.* **31**, 998–1004 (2008).
- Martinez, F. J. et al. A new approach for identifying patients with undiagnosed chronic obstructive pulmonary disease. *Am. J. Respir. Crit. Care Med.* **195**, 748–756 (2017).
- Strug, L. J. et al. Cystic fibrosis gene modifier SLC26A9 modulates airway response to CFTR-directed therapeutics. *Hum. Mol. Genet.* **25**, 4590–4600 (2016).

Acknowledgements

This research has been conducted using the UK Biobank Resource under applications 648, 4892 and 26041. L. Wain holds a GSK/British Lung Foundation Chair in Respiratory Research. M. Tobin is supported by a Wellcome Trust Investigator Award (WT202849/Z/16/Z). M. Tobin and L. Wain have been supported by the Medical Research Council (MRC) (MR/N011317/1). The research was partially supported by the National Institute for Health Research (NIHR) Leicester Biomedical Research Centre; the views expressed are those of the author(s) and not necessarily those of the National Health Service (NHS), the NIHR or the Department of Health. I.H. was partially supported by the NIHR Nottingham Biomedical Research Centre; the views expressed are those of the author(s) and not necessarily those of the NHS, the NIHR or the Department of Health. This research used the ALICE and SPECTRE High Performance Computing Facilities at the University of Leicester. Additional acknowledgments and funding details for other co-authors and contributing studies (including the SpiroMeta consortium) are in the Supplementary Note.

Author contributions

All authors critically reviewed the manuscript before submission. K.S., U.S.S.G., S.K., S.M.K., T.L., P.S.B., T.H.B., E.R.B., Y.B., Z.C., J.D.C., J.D., D.L.D., C.G., A.G., K.H., J.D.H., J.E.H., P.J., C.L., L.Li, N.L., J.C.M., H.R., I.Sayers, D.D.S., R.T.-S., J.C.W., P.G.W., L.M.Y., O.T.R., M.K., O.P., U.G., I.R., I.J.D., N.M.P., H.S., A.L.J., J.F.W., E.Z., M.J., N.W., A.S.B., R.A.S., D.A.M., M.H.C., D.P.S., I.P.H., M.D.T. and L.V.W. contributed to the conception and design of the study. N.S., A.L.G., A.M.E., V.E.J., B.D.H., C.A.M., C.Batini, K.A.F., K.S., P.S., Xingnan Li, R.B., N.E.R., M.O., J.Zhao, M.W., S.W., K.A.K., J.P.C., B.B.S., J.Zhou, J.H., M.I., S.E.H., J.M., S.E., I.Surakka, V.V., T.L., R.J.A., F.D., J.D.H., P.K.J., Xuan Li, A.Mahajan, J.C.M., D.C.N., M.M.P., D.P., D.Q., R.R., H.R., D.S., P.R.H.J.T., M.V., L.M.Y., O.G.T., N.M.P., N.W., E.K.S., C.H., A.P.M., A.S.B., R.A.S., M.H.C., D.P.S., M.D.T. and L.V.W. undertook data analysis. N.S., A.L.G., A.M.E., V.E.J., C.A.M., C.Batini, K.A.F., K.S., P.S., Xingnan Li, N.E.R., M.O., M.W., K.A.K., B.B.S., S.K., M.I., R.J.A., C.Brandsma, J.D., F.D., R.E., C.G., A.G., A.L.H., J.D.H., G.H., P.K.J., C.L., Xuan Li, K.L., L.Lind, J.L., J.C.M., A.Murray, R.P., M.M.P., M.L.P., D.J.P., D.P., D.Q., R.R., H.R., I.Sayers, B.H.S., M.S., L.M.Y., O.G.T., N.M.P., H.S., J.F.W., B.S., M.J., N.W., C.H., A.P.M., A.S.B., R.A.S., R.G.W., M.H.C., D.P.S., I.P.H., M.D.T. and L.V.W. contributed to data acquisition and/or interpretation. N.S., A.L.G., A.M.E., I.P.H., M.D.T. and L.V.W. drafted the manuscript.

Competing interests

The following authors report potential conflicts of interest: K.S. is an employee of GlaxoSmithKline (GSK) and may own company stock. Z.C. reports grants from GSK and Merck. J.D. reports personal fees and nonfinancial support from Merck Sharp & Dohme (MSD) and Novartis, and grants from British Heart Foundation, European Research Council, MSD, NIHR, NHS Blood and Transplant, Novartis, Pfizer, UK MRC, Wellcome Trust and AstraZeneca. J.D.H. is an employee of GlaxoSmithKline and may own company stock. N.L. is an employee and shareholder of GSK. J.C.M. was a Merck employee during this study, and is now a Celgene employee. D.C.N. has been a Merck

& Co. employee during this study and is now an employee at Biogen Inc. H.R. has been a Merck & Co. employee during this study and is now an employee at Biogen Inc. I.S. has received support from GSK and Boehringer Ingelheim. R.T.-S. is an employee and shareholder of GlaxoSmithKline. M.v.d.B. reports grants paid to the University from AstraZeneca, TEVA, GSK and Chiesi outside the submitted work. J.C.W. is an employee of GSK and may own company stock. L.M.Y.-A. is an employee of GSK and may own company stock. For H.S., Helmholtz Center Munich is funded by the German Federal Ministry of Education and Research (BMBF) and by the State of Bavaria, Competence Network Asthma and COPD (ASCONET), network COSYCONET (subproject 2, BMBF FKZ 01G10882), funded by the BMBF. In the past three years, E.K.S. received honoraria from Novartis for Continuing Medical Education Seminars and grant and travel support from GlaxoSmithKline. A.S.B. reports grants from Merck, Pfizer, Novartis, Biogen and AstraZeneca and personal fees from Novartis. R.A.S. is an employee and shareholder in GSK. R.G.W. reports that the China Kadoorie Biobank study has received grant support from GSK. M.H.C. has received grant support from GSK. I.P.H. has funded research collaborations with GSK, Boehringer Ingelheim and Orion. M.D.T. receives funding from GSK for a collaborative research project outside of the submitted work. L.V.W. receives funding from GSK for a collaborative research project outside of the submitted work.

Additional information

Supplementary information is available for this paper at <https://doi.org/10.1038/s41588-018-0321-7>.

Reprints and permissions information is available at www.nature.com/reprints.

Correspondence and requests for materials should be addressed to M.D.T. or L.V.W.

Publisher's note: Springer Nature remains neutral with regard to jurisdictional claims in published maps and institutional affiliations.

© The Author(s), under exclusive licence to Springer Nature America, Inc. 2019

¹Department of Health Sciences, University of Leicester, Leicester, UK. ²Population Health and Immunity Division, The Walter and Eliza Hall Institute of Medical Research, Parkville, Victoria, Australia. ³Department of Medical Biology, University of Melbourne, Parkville, Victoria, Australia. ⁴Channing Division of Network Medicine, Brigham and Women's Hospital, Boston, MA, USA. ⁵Division of Pulmonary and Critical Care Medicine, Brigham and Women's Hospital, Boston, MA, USA. ⁶Target Sciences, GlaxoSmithKline, Collegeville, PA, USA. ⁷Department of Medicine, Faculty of Medicine Siriraj Hospital, Mahidol University, Bangkok, Thailand. ⁸Division of Genetics, Genomics and Precision Medicine, Department of Medicine, University of Arizona, Tucson, AZ, USA. ⁹Nuffield Department of Population Health, University of Oxford, Oxford, UK. ¹⁰Medical Research Council Population Health Research Unit, University of Oxford, Oxford, UK. ¹¹The University of British Columbia Centre for Heart Lung Innovation, St Paul's Hospital, Vancouver, British Columbia, Canada. ¹²Cardiovascular Epidemiology Unit, Department of Public Health and Primary Care, University of Cambridge, Cambridge, UK. ¹³Department of Epidemiology and Biostatistics, MRC-PHE Centre for Environment & Health, School of Public Health, Imperial College London, London, UK. ¹⁴A list of members and affiliations appears in Supplementary Note. ¹⁵Interfaculty Institute for Genetics and Functional Genomics, Department of Functional Genomics, University Medicine Greifswald, Greifswald, Germany. ¹⁶Centre for Global Health Research, Usher Institute for Population Health Sciences and Informatics, University of Edinburgh, Edinburgh, UK. ¹⁷Centre for Cardiovascular Sciences, Queen's Medical Research Institute, University of Edinburgh, Edinburgh, UK. ¹⁸Department of Biostatistics, University of Liverpool, Liverpool, UK. ¹⁹MRC/BHF Cardiovascular Epidemiology Unit, Department of Public Health and Primary Care, University of Cambridge, Cambridge, UK. ²⁰Flatiron Institute, Simons Foundation, New York, NY, USA. ²¹Busselton Population Medical Research Institute, Sir Charles Gairdner Hospital, Nedlands, Western Australia, Australia. ²²School of Population Health, The University of Western Australia, Crawley, Western Australia, Australia. ²³PathWest Laboratory Medicine of WA, Sir Charles Gairdner Hospital, Crawley, Western Australia, Australia. ²⁴School of Pathology and Laboratory Medicine, The University of Western Australia, Crawley, Western Australia, Australia. ²⁵Institute of Epidemiology, Helmholtz Zentrum Muenchen—German Research Center for Environmental Health, Neuherberg, Germany. ²⁶Institute and Outpatient Clinic for Occupational, Social and Environmental Medicine, Ludwig-Maximilians-Universität, Munich, Germany. ²⁷Comprehensive Pneumology Center Munich (CPC-M), Member of the German Center for Lung Research (DZL), Munich, Germany. ²⁸Swiss Tropical and Public Health Institute, Basel, Switzerland. ²⁹University of Basel, Basel, Switzerland. ³⁰Centre for Cognitive Ageing and Cognitive Epidemiology, University of Edinburgh, Edinburgh, UK. ³¹Centre for Genomic and Experimental Medicine, Institute of Genetics & Molecular Medicine, University of Edinburgh, Edinburgh, UK. ³²Medical Research Council Human Genetics Unit, Institute of Genetics and Molecular Medicine, University of Edinburgh, Edinburgh, UK. ³³Department of Immunology, Genetics and Pathology, Science for Life Laboratory, Uppsala Universitet, Uppsala, Sweden. ³⁴Institute for Molecular Medicine Finland (FIMM), University of Helsinki, Helsinki, Finland. ³⁵The National Institute for Health and Welfare (THL), Helsinki, Finland. ³⁶Department of Clinical Chemistry, Fimlab Laboratories, and Finnish Cardiovascular Research Center - Tampere, Faculty of Medicine and Life Sciences, University of Tampere, Tampere, Finland. ³⁷Department of Clinical Science, University of Bergen, Bergen, Norway. ³⁸Department of Epidemiology, Johns Hopkins University School of Public Health, Baltimore, MD, USA. ³⁹Department of Molecular Medicine, Laval University, Québec, Canada. ⁴⁰Institut Universitaire de Cardiologie et de Pneumologie de Québec, Laval University, Québec, Canada. ⁴¹University of Groningen, University Medical Center Groningen, Department of Pathology and Medical Biology, GRIAC Research Institute, University of Groningen, Groningen, The Netherlands. ⁴²National Jewish Health, Denver, CO, USA. ⁴³Division of Pulmonary, Critical Care and Sleep Medicine, National Jewish Health, Denver, CO, USA. ⁴⁴British Heart Foundation Cambridge Centre of Excellence, Division of Cardiovascular Medicine, Addenbrooke's Hospital, Cambridge, UK. ⁴⁵Department of Human Genetics, Wellcome Trust Sanger Institute, Cambridge, UK. ⁴⁶NIHR Blood and Transplant Research Unit in Donor Health and Genomics, Department of Public Health and Primary Care, University of Cambridge, Cambridge, UK. ⁴⁷Department of Internal Medicine B - Cardiology, Intensive Care, Pulmonary Medicine and Infectious Diseases, University Medicine Greifswald, Greifswald, Germany. ⁴⁸Research Unit of Molecular Epidemiology, Institute of Epidemiology, Helmholtz Zentrum Muenchen - German Research Center for Environmental Health, Neuherberg, Germany. ⁴⁹Centre for Environmental Health & Sustainability, University of Leicester, Leicester, UK. ⁵⁰UK Small Area Health Statistics Unit, MRC-PHE Centre for Environment and Health, School of Public Health, Imperial College London, London, UK. ⁵¹Imperial College Healthcare NHS Trust, St Mary's Hospital, London, UK. ⁵²Department of Genetics and Genomic Sciences, Icahn School of Medicine at Mount Sinai, New York, NY, USA. ⁵³Department of Epidemiology, University of Colorado Anschutz Medical Campus, Aurora, CO, USA. ⁵⁴Department of Molecular Biology, Medical Biochemistry, and Pathology, Laval University, Québec, Canada. ⁵⁵MRC Epidemiology Unit, University of Cambridge School of Clinical Medicine, Cambridge, UK. ⁵⁶Department of Epidemiology & Biostatistics, Peking University Health Science Center, Beijing, China. ⁵⁷Department of

Medical Sciences, Cardiovascular Epidemiology, Uppsala University, Uppsala, Sweden. ⁵⁸GSK R&D, Collegeville, PA, USA. ⁵⁹Wellcome Trust Centre for Human Genetics, University of Oxford, Oxford, UK. ⁶⁰MRL, Merck & Co., Inc, Kenilworth, NJ, USA. ⁶¹The Institute of Medical Sciences, Aberdeen Biomedical Imaging Centre, University of Aberdeen, Aberdeen, UK. ⁶²Gossamer Bio, San Diego, CA, USA. ⁶³Institute of Epidemiology and Social Medicine, University of Münster, Münster, Germany. ⁶⁴Division of Respiratory Medicine and NIHR-Nottingham Biomedical Research Centre, University of Nottingham, Nottingham, UK. ⁶⁵Respiratory Division, Department of Medicine, University of British Columbia, Vancouver, British Columbia, Canada. ⁶⁶Division of Population Health and Genomics, Ninewells Hospital and Medical School, University of Dundee, Dundee, UK. ⁶⁷Psychiatric Genetics Unit, Group of Psychiatry, Mental Health and Addiction, Vall d'Hebron Research Institute (VHIR), Universitat Autònoma de Barcelona, Barcelona, Spain. ⁶⁸Department of Psychiatry, Hospital Universitari Vall d'Hebron, Barcelona, Spain. ⁶⁹Biomedical Network Research Centre on Mental Health (CIBERSAM), Instituto de Salud Carlos III, Barcelona, Spain. ⁷⁰VA Boston Healthcare System, Boston, MA, USA. ⁷¹Department of Medicine, Boston University School of Medicine, Boston, MA, USA. ⁷²University of Groningen, University Medical Center Groningen, Department of Pulmonology, GRIAC Research Institute, University of Groningen, Groningen, The Netherlands. ⁷³Target Sciences - R&D, GSK Medicines Research Centre, Stevenage, UK. ⁷⁴UCSF Pulmonary, Critical Care, Allergy and Sleep Medicine, University of California, San Francisco, CA, USA. ⁷⁵Department of Computer Science, Princeton University, Princeton, NJ, USA. ⁷⁶Lewis-Sigler Institute for Integrative Genomics, Princeton University, Princeton, NJ, USA. ⁷⁷Department of Clinical Physiology and Nuclear Medicine, Turku University Hospital, Turku, Finland. ⁷⁸Research Centre of Applied and Preventive Cardiovascular Medicine, University of Turku, Turku, Finland. ⁷⁹Department of Clinical Physiology, Tampere University Hospital, and Finnish Cardiovascular Research Center - Tampere, Faculty of Medicine and Life Sciences, University of Tampere, Tampere, Finland. ⁸⁰University of Split School of Medicine, Split, Croatia. ⁸¹Department of Psychology, University of Edinburgh, Edinburgh, UK. ⁸²Department of Pulmonary Physiology and Sleep Medicine, Sir Charles Gairdner Hospital, Nedlands, Western Australia, Australia. ⁸³School of Medicine and Pharmacology, The University of Western Australia, Crawley, Western Australia, Australia. ⁸⁴Wellcome Sanger Institute, Hinxton, UK. ⁸⁵Institute of Translational Genomics, Helmholtz Zentrum Muenchen - German Research Center for Environmental Health, Neuherberg, Germany. ⁸⁶Center for Life Course Health Research, Faculty of Medicine, University of Oulu, Oulu, Finland. ⁸⁷Biocenter Oulu, University of Oulu, Oulu, Finland. ⁸⁸Unit of Primary Health Care, Oulu University Hospital, Oulu, Finland. ⁸⁹Department of Life Sciences, College of Health and Life Sciences, Brunel University London, Uxbridge, UK. ⁹⁰Population Health Research Institute, St George's, University of London, London, UK. ⁹¹National Institute for Health Research, Leicester Respiratory Biomedical Research Centre, Glenfield Hospital, Leicester, UK. ⁹²These authors contributed equally: N. Shrine, A. L. Guyatt, A. M. Erzurumluoglu, I. P. Hall, M. D. Tobin, L. V. Wain. *e-mail: mt47@leicester.ac.uk; lvw1@leicester.ac.uk

Methods

Study design overview and rationale. For the two-stage approach, we first selected distinct signals of association (defined using conditional analyses) with one or more traits achieving $P < 5 \times 10^{-9}$ in UK Biobank only (maximum $n = 321,047$). A threshold of $P < 5 \times 10^{-9}$ was selected to maximize stringency and for consistency with currently recommended genome-wide significance thresholds for resequencing analyses of European-ancestry individuals²³. We reported as new those signals that additionally met $P < 10^{-3}$ in SpiroMeta (effective $n > 70\%$ of n up to 79,055; see Supplementary Note and Supplementary Fig. 7 for power calculations), with consistent directions of effect. We term these tier 1 signals, as they meet our highest level of stringency. Methods for conditional analyses and determining novelty are described below.

For the one-stage approach, we selected distinct signals of association (defined using conditional analyses) with one or more traits reaching $P < 5 \times 10^{-9}$ in the meta-analysis of UK Biobank and SpiroMeta (maximum $n = 400,102$), reporting as new those with a consistent direction of effect that additionally met $P < 10^{-3}$ in both UK Biobank and SpiroMeta. We term these signals tier 2, as they meet our second-highest level of stringency.

All signals meeting either set of criteria described above, and that had not been previously published, were reported as new association signals for lung function. Signals that reached $P < 5 \times 10^{-9}$ in the meta-analysis of UK Biobank and SpiroMeta, had a consistent direction of effect in UK Biobank and SpiroMeta, and that did not reach $P < 10^{-3}$ in both UK Biobank and SpiroMeta are presented as tier 3, and were not included in further analyses.

Data for chromosome X were available for 321,027 European individuals in UK Biobank and 38,199 individuals from SpiroMeta (1000 Genomes Project Phase 1 imputation)³⁵.

Please see the Life Sciences Reporting Summary.

UK Biobank. The UK Biobank resource is described elsewhere (see URLs). Individuals were selected for inclusion in this study if they (1) had complete data for age, sex, height and smoking status; (2) had spirometry meeting quality control requirements (based on analyses of acceptability, reproducibility and blow curve metrics; Supplementary Note); (3) had genome-wide imputed data and (4) were of European ancestry based on genetic data (Supplementary Note and Supplementary Fig. 1). Genotyping was undertaken using the Affymetrix Axiom UK BiLEVE and UK Biobank arrays¹³. Genotypes were imputed to the Haplotype Reference Consortium panel³⁶ (Supplementary Note), and retained if minor allele count was ≥ 3 and imputation quality (info) was > 0.5 . In total, 321,047 individuals were included in our analyses (Supplementary Table 1).

Residuals from linear regression of each trait (FEV_1 , FVC, FEV_1/FVC and PEF) against age, age², sex, height, smoking status (ever or never) and genotyping array were ranked and inverse-normal transformed, giving normally distributed Z-scores. These Z-scores were used for genome-wide association testing under an additive genetic model using BOLT-LMM v2.3 (ref. ²⁰). Principal components were not included as BOLT-LMM uses a linear mixed model to account for relatedness and fine-scale population structure.

LD score regression implemented in LDSC²¹ was used to estimate test statistic inflation due to any confounding of the association between lung function and genotype, e.g., by population stratification. Genomic control was applied, adjusting test statistics by LD score regression intercepts: 1.12 for FEV_1 , 1.14 for FVC, 1.19 for FEV_1/FVC and 1.13 for PEF (Supplementary Fig. 8 and Supplementary Table 27), acknowledging that this might be overly conservative for UK Biobank.

SpiroMeta consortium. The SpiroMeta consortium meta-analysis comprised 79,055 individuals from 22 studies. Some 13 studies ($n = 21,436$) were imputed to the 1000 Genomes Project Phase 1 panel³⁵ (B58C, BHS1&2, three Croatian studies (CROATIA-Korcula, CROATIA-Split and CROATIA-Vis), Health 2000, KORA F4, KORA S3, LBC1936, NSPHS, ORCADES, SAPALDIA and YFS) and 9 studies ($n = 61,682$) were imputed to the Haplotype Reference Consortium panel³⁷ (EPIC (obese cases and population-based studies), GS:SFHS, NFBC1966, NFBC1986, PIVUS, SHIP, SHIP-TREND, UKHLS and VIKING). See Supplementary Tables 2 and 3 for abbreviation definitions, study characteristics, and details of genotyping platforms, imputation panels and methods). Measurements of spirometry for each study are described in Supplementary Note.

In each study, linear regression models were fitted for each trait (FEV_1 , FEV_1/FVC , FVC and, where available, PEF), with adjustment for age, age², sex and height. For studies with unrelated individuals, models were fitted separately in ever and never smokers, with additional adjustment for ancestral principal components. Studies with related individuals fitted mixed models in all individuals to account for relatedness, with ever smoking status as a covariate.

In all studies, residuals were rank-based inverse normal-transformed and used as the phenotype for association testing, under an additive genetic model (Supplementary Table 3).

In the study-level results, variants were excluded if they had a low minor allele count (Supplementary Table 3) or imputation quality (info) of < 0.3 . In studies of unrelated individuals, ever and never smokers' results were combined using inverse-variance-weighted meta-analysis. Genomic control was applied to all study-level results, before combining results across all studies using

inverse-variance-weighted meta-analysis. LD score regression intercepts for the meta-analysis were close to 1.00 (Supplementary Fig. 8 and Supplementary Table 27), therefore genomic control was not applied.

Meta-analyses. A total of 19,819,130 variants (imputed or genotyped) in both UK Biobank and SpiroMeta were meta-analyzed, using inverse-variance-weighted fixed-effect meta-analysis. No further genomic control was applied as LD score regression intercepts were close to 1.00 (Supplementary Table 27).

Selection of new signals using conditional analyses. All SNPs ± 1 Mb from each sentinel variant were extracted. We performed stepwise conditional analysis to select independently associated SNPs within each 2-Mb region, using GCTA⁵⁸. LD was estimated for UK Biobank from the same individuals used in discovery, and for SpiroMeta, from an unrelated subset of 48,943 UK Biobank individuals¹⁸. Secondary signals identified within each 2-Mb region were required to meet tier 1 or tier 2 criteria (described above) after conditioning on the primary sentinel variant. A combined list of distinct lung function signals was then made across the four phenotypes, FEV_1 , FVC, FEV_1/FVC and PEF, as follows: where sentinel variants for two signals for different phenotypes were in high LD ($r^2 > 0.5$), we retained the most significant variant; where two signals were in moderate LD ($0.1 > r^2 > 0.5$), we retained variants if, after conditional analysis, they still met the tier 1 or tier 2 threshold; for signals in low LD ($r^2 < 0.1$) we retained both variants. We then used the same criteria to identify a subset of new signals that were distinct from previously published independent signals (see below).

Assessment of previously reported lung function signals. We identified 184 autosomal signals from previous GWASs of lung function and COPD^{14–14}. After LD pruning (keeping only signals with LD of $r^2 < 0.1$), we removed 24 nonindependent SNPs, leaving 160 previously reported independent signals. Of six previously reported signals in the HLA region, we included only the three independent lung function HLA signals reported from conditional analysis using all imputed HLA genotypes¹⁸: *AGER* (rs2070600), *HLA-DQB1* (rs114544105) and near *ZNF184* (rs34864796), leaving 157 autosomal signals.

We confirmed association of previously reported signals in our data if they met any of three criteria: (1) the previously reported sentinel was associated ($P < 10^{-5}$) with any lung function trait in UK Biobank; (2) a proxy for the previously reported sentinel with $r^2 > 0.5$ was associated ($P < 10^{-5}$) with any lung function trait in UK Biobank; or (3) a proxy for the previously reported sentinel with $r^2 > 0.1$ was associated with any lung function trait meeting tier 1 or tier 2 criteria (Supplementary Fig. 3).

Effect of genetic risk score on COPD susceptibility in multiple ancestries.

To test association of all lung function signals with COPD susceptibility, we constructed a 279-variant weighted GRS comprising the 139 novel and 140 previously reported signals; we used the previously reported sentinel SNP for published signals. Weights were derived using the FEV_1/FVC -decreasing (generally COPD risk-increasing) alleles. For previously reported signals ($n = 140$), effect sizes from UK Biobank were used as weights for the 94 signals that were not discovered using UK Biobank data. Weights were taken from SpiroMeta for 46 signals whose discovery included UK Biobank. For novel signals, weights were taken from SpiroMeta for two-stage (tier 1) signals ($n = 99$), and the smallest absolute effect size from either UK Biobank or SpiroMeta was used for one-stage (tier 2) signals ($n = 40$) (Supplementary Table 28). This approach was taken to derive conservative weights, thus reducing the likelihood of bias by winner's curse. For the weighted GRS the number of risk alleles at each variant was multiplied by its weight.

The GRS was first calculated in unrelated individuals (KING kinship coefficient of < 0.0884) within six ancestral groups of UK Biobank: Europeans, South Asians, Africans, Chinese, mixed African and Europeans, and mixed other (total sample of unrelated individuals across six ancestries: 323,001) using PLINK. Weights were calculated and allele counts were summed as described above. COPD was defined as $FEV_1/FVC < 0.7$ and $FEV_1 < 80\%$ predicted, that is, GOLD stage 2–4 categorization. Associations with the GRS were then tested using COPD (in ancestral groups with at least 100 COPD cases) and FEV_1/FVC as the outcomes.

We also calculated the GRS in individuals from the CKB. Four of the 279 SNPs were unavailable in CKB (rs1800888, rs56196860, rs72724130 and rs77672322), and for 12 SNPs, proxies were used (minimum $r^2 = 0.3$). Analyses were undertaken in all COPD GOLD stage 2–4 cases ($FEV_1/FVC < 0.7$ and $FEV_1 < 0.8$ of the predicted value: 6,013 cases and 69,567 controls), against an unbiased set of population controls. The GRS was also tested for association with FEV_1/FVC in CKB ($n = 72,796$).

Logistic regression of COPD case-control status with the GRS in UK Biobank and CKB assumed an additive genetic effect and was adjusted for age, age², sex, height, and smoking (Supplementary Table 19). Ten principal components were included in UK Biobank analyses. In CKB, analyses were stratified by geographical regions, and then meta-analyzed using an inverse-variance fixed effect model. Linear models assessing the association with FEV_1/FVC were fitted using the transformed outcome used in the main GWAS analysis.

We then tested association in five European-ancestry COPD case-control studies: COPDGene (non-Hispanic white population) (3,068 cases, 2,110 controls), ECLIPSE (1,713 cases, 147 controls), GenKOLS (836 cases, 692 controls), NETT-NAS (374 cases, 429 controls) and SPIROMICS (988 cases, 537 controls) (Supplementary Table 20). We also tested this GRS in the COPDGene African-American population study (910 cases, 1,556 controls). Logistic regression models using COPD as outcome and the GRS as exposure were adjusted for age, age², sex, height, and principal components (Supplementary Table 21 and Supplementary Fig. 9). Single-variant associations of the 279 SNPs with COPD are in Supplementary Table 29.

Next, we divided individuals in the external COPD case-control studies into deciles, according to their values of the weighted GRS (undertaken separately by study group). For each of deciles 2–10, logistic models were fitted, comparing the risk of COPD for members of the given decile compared to those in the lowest decile (i.e., decile 1, the decile containing those with lowest values of the weighted GRS). Covariates were the same as for COPD analyses. Results were combined across European-ancestry study groups by fixed-effect meta-analysis (Supplementary Table 22).

Effects on smoking behavior. As our discovery GWAS in UK Biobank was adjusted for ever-smoking status, and not for pack years of smoking (this information was missing for 32% of smokers), we evaluated whether any lung function association signals might be driven by an association with smoking behavior by testing for association with smoking initiation (123,890 ever smokers versus 151,706 never smokers) and cigarettes per day ($n = 80,015$) in UK Biobank (see Supplementary Note). We also tested for association with lung function in never smokers only ($n = 173,658$). We excluded signals associated with smoking behavior (Supplementary Table 6) but not with lung function in never smokers.

Smoking interaction. For associated variants (new and previously reported), we repeated association testing for lung function separately in UK Biobank and SpiroMeta (up to 176,701 ever smokers and 197,999 never smokers), and tested for an interaction effect with smoking using the Welch test (Supplementary Note). A threshold of $P < 1.79 \times 10^{-4}$ (Bonferroni-corrected for 279 tests) indicated significance.

We also tested for interaction between the weighted GRS and smoking within 303,619 unrelated individuals of European ancestry in UK Biobank, using COPD and FEV₁/FVC as outcomes (FEV₁/FVC was preadjusted for age, age², sex and height, and the residuals transformed as per the main GWAS analysis). For COPD (defined as FEV₁/FVC < 0.7, and FEV₁ < 80% predicted) a logistic model was fitted:

COPD ~ genotyping array + 10 principal components + age + age² + sex + height + smoking status + weighted risk score + (smoking status × weighted risk score).

For FEV₁/FVC, a linear model was fitted:

FEV₁/FVC ~ genotyping array + 10 principal components + smoking status + weighted risk score + (smoking status × weighted risk score).

Proportion of variance explained. We calculated the proportion of variance explained by the previously reported ($n = 140$) and new ($n = 139$) variants associated with lung function using the formula:

$$\frac{\sum_{i=1}^n 2f_i(1-f_i)\beta_i^2}{V}$$

where n is the number of variants, f_i and β_i are the frequency and effect estimate of the i th variant, and V is the phenotypic variance (which was always 1 as our phenotypes were inverse-normal transformed). We used the same conservative effect estimates (β) as GRS weights for the 279 GRS variants, derived from either UK Biobank or SpiroMeta effect estimates (described above). Our previously published estimate of proportion of variance explained¹⁸ used UK Biobank effect estimates. We assumed a heritability of 40% (refs. ^{24,25}) to estimate the proportion of additive polygenic variance.

Fine-mapping. A Bayesian method⁵⁹ was used to fine-map lung-function-associated signals to the set of variants that were 99% probable to contain the underlying causal variant (assuming that the causal variant was analyzed). This was undertaken for new signals and for previously reported signals reaching $P < 10^{-5}$ in UK Biobank. For previously reported signals, the sentinel variant from the current UK Biobank analysis was used, instead of the previously reported variant. We used a value of 0.04 for W (the variance of the prior distribution of effect sizes) in the approximate Bayes factor formula⁶⁰. Effect sizes and standard errors for fine-mapping were obtained from inverse-variance-weighted meta-analysis of UK Biobank and SpiroMeta (maximum $n = 400,102$). Signals in the HLA region were not included.

Implication of potentially causal genes. Annotation of deleterious variants. Variants in the 99% credible sets were checked for predicted functional effect if they were annotated as exonic, splicing, ncRNA_exonic, 5′-untranslated region (5′-UTR) or 3′-UTR by ANNOVAR⁶¹. We then used SIFT, PolyPhen-2 (implemented using the Ensembl GRCh37 Variant Effect Predictor, see URLs)

and FATHMM⁶² to annotate missense variants, and CADD (also implemented using VEP) to annotate noncoding variation. Variants were annotated as deleterious if they were labeled deleterious by SIFT, probably damaging or possibly damaging by PolyPhen-2, damaging by FATHMM (specifying the “Inherited Disease” option of the “Coding Variants” method, and using the “Unweighted” prediction algorithm) or had a CADD scaled score ≥ 20 (ref. ¹⁸). The union of the four methods was taken to establish the number of potentially deleterious variants and their unique genes.

Gene expression and protein levels. At 276 of 279 (3 HLA signals excluded) signals, the sentinel variant and 99% credible set⁵⁹ were used to query three eQTL resources: lung eQTL ($n = 1,111$)¹³, blood eQTL ($n = 4,896$)⁶³ and GTEx (V7; with maximum $n = 388$, depending on tissue: artery aorta ($n = 267$), artery coronary ($n = 152$), artery tibial ($n = 388$), colon sigmoid ($n = 203$), colon transverse ($n = 246$), esophagus gastroesophageal junction ($n = 213$), esophagus muscularis ($n = 335$), lung ($n = 383$), small intestine terminal ileum ($n = 122$), stomach ($n = 237$) and whole blood ($n = 369$)⁶⁴, and one blood pQTL resource ($n = 3,301$)³⁹.

A gene was classified as a putative causal gene if the sentinel SNP or any SNP in the respective 99% credible set was associated with expression of this gene or its protein levels (FDR < 5% for eQTL, $P < 5.03 \times 10^{-8}$ for pQTL (276 tests at 3,600 proteins)) and if the GWAS sentinel SNP or any SNP in the respective 99% credible set was the variant most strongly associated with expression of the respective gene or level of the respective protein (that is, the sentinel eQTL/pQTL SNP) in one or more of the eQTL and pQTL data sets.

Pathway analysis. We tested for enrichment of genes identified via functional annotation, gene expression or protein level analyses in pathway and gene set ontology databases using ConsensusPathDB⁶⁵. Pathways or gene sets represented entirely by genes implicated by the same association signal were excluded. Gene sets and pathways with FDR < 5% are reported.

Functional enrichment analyses. We carried out stratified LD score regression to identify significant enrichment of heritability at variants overlapping histone marks (for example H3K4me1 and H3K4me3) specific to lung, fetal lung and smooth muscle-containing (for example, colon or stomach) cell lines, using methods specified by Finucane et al.⁴⁰

We separately selected FEV₁/FVC and FVC associated SNPs passing two thresholds ($P < 5 \times 10^{-5}$ and $P < 5 \times 10^{-9}$ in the meta-analysis) as input to GARFIELD⁴¹ to test for enrichment of our signals for 424 DNase I hypersensitive site hotspot annotations derived from 55 different tissues in the RoadMap Epigenomics and ENCODE projects.

Using DeepSEA⁴², we analyzed all SNPs in the 99% credible set for predicted chromatin effects. We reported effects for any chromatin effect and lung-related cell line with an E-value < 0.05 (that is, the expected proportion of SNPs with a larger predicted effect based on empirical distributions of predicted effects for 1000 Genomes SNPs) and an absolute difference in probability of > 0.1 (threshold for ‘high confidence’) between the reference and alternative allele.

Drug targets. Genes identified as potentially causal using eQTL, pQTL or variant annotation were interrogated against the gene-drug interactions table of the Drug-Genes Interactions Database (see URLs). Drugs were mapped to ChEMBL IDs (see URLs), and indications (MeSH headings) were added.

Phenome-wide association studies. To identify whether the 279 signals were associated with other traits and diseases, the weighted GRS was calculated in up to 379,337 UK Biobank samples, and a PheWAS was performed, with the GRS as the exposure. Traits included UK Biobank baseline measures (from questionnaires and physical measures), self-reported medication usage, and operative procedures, as well as those captured in Office of Population Censuses and Surveys codes from the electronic health record. We also included self-reported disease variables and those from hospital episode statistics (ICD-10 codes truncated to three-character codes and combined in block and chapter groups), combining these where possible to maximize power. The GRS analysis included 2,453 traits, and the single-variant analysis contained 2,411 traits (traits with > 200 cases were included for the single-variant PheWAS, whereas traits with > 50 cases were included in the GRS PheWAS). Analyses were conducted in unrelated European-ancestry individuals (KING kinship coefficient < 0.0442), and were adjusted for age, sex, genotyping array and ten principal components. Logistic and linear models were fitted for binary and quantitative outcomes, respectively. FDRs were calculated according to the number of traits in the GRS and single-variant PheWAS (2,453 or 2,411, respectively).

In addition, the sentinel variants 99% credible set variants were queried against the GWAS catalog⁶⁶ (see URLs) and GRASP⁶⁷ (see URLs) for associations at $P < 5 \times 10^{-8}$. Associations relating to methylation, expression, metabolite or protein levels, lung function or COPD were not included.

Reporting Summary. Further information on research design is available in the Nature Research Reporting Summary linked to this article.

Data availability

SpiroMeta GWAS summary statistics and UK Biobank GWAS summary statistics are available online via LD-Hub (<http://ldsc.broadinstitute.org/ldhub/>). Single-variant PheWAS results are available by request to the corresponding authors. The newly derived spirometry variables are available from UK Biobank (<http://www.ukbiobank.ac.uk/>).

References

55. The 1000 Genomes Project Consortium. A map of human genome variation from population-scale sequencing. *Nature* **467**, 1061 (2010).
56. Bycroft, C. et al. Genome-wide genetic data on ~500,000 UK Biobank participants. Preprint at <https://www.biorxiv.org/content/early/2017/07/20/166298> (2017).
57. McCarthy, S. et al. A reference panel of 64,976 haplotypes for genotype imputation. *Nat. Genet.* **48**, 1279–1283 (2016).
58. Yang, J., Lee, S. H., Goddard, M. E. & Visscher, P. M. GCTA: a tool for genome-wide complex trait analysis. *Am. J. Hum. Genet.* **88**, 76–82 (2011).
59. Wakefield, J. Reporting and interpretation in genome-wide association studies. *Int. J. Epidemiol.* **37**, 641–653 (2008).
60. van de Bunt, M., Cortes, A., Brown, M. A., Morris, A. P. & McCarthy, M. I. Evaluating the performance of fine-mapping strategies at common variant GWAS loci. *PLoS Genet.* **11**, e1005535 (2015).
61. Wang, K., Li, M. & Hakonarson, H. ANNOVAR: functional annotation of genetic variants from high-throughput sequencing data. *Nucleic Acids Res.* **38**, e164 (2010).
62. Shihab, H. A. et al. Predicting the functional, molecular, and phenotypic consequences of amino acid substitutions using hidden Markov models. *Hum. Mutat.* **34**, 57–65 (2013).
63. Jansen, R. et al. Conditional eQTL analysis reveals allelic heterogeneity of gene expression. *Hum. Mol. Genet.* **26**, 1444–1451 (2017).
64. Battle, A., Brown, C. D., Engelhardt, B. E. & Montgomery, S. B. Genetic effects on gene expression across human tissues. *Nature* **550**, 204–213 (2017).
65. Kamburov, A., Stelzl, U., Lehrach, H. & Herwig, R. The ConsensusPathDB interaction database: 2013 update. *Nucleic Acids Res.* **41**, D793–D800 (2013).
66. MacArthur, J. et al. The new NHGRI-EBI Catalog of published genome-wide association studies (GWAS Catalog). *Nucleic Acids Res.* **45**, D896–D901 (2017).
67. Leslie, R., O'Donnell, C. J. & Johnson, A. D. GRASP: analysis of genotype-phenotype results from 1390 genome-wide association studies and corresponding open access database. *Bioinformatics* **30**, i185–i194 (2014).

Reporting Summary

Nature Research wishes to improve the reproducibility of the work that we publish. This form provides structure for consistency and transparency in reporting. For further information on Nature Research policies, see [Authors & Referees](#) and the [Editorial Policy Checklist](#).

Statistical parameters

When statistical analyses are reported, confirm that the following items are present in the relevant location (e.g. figure legend, table legend, main text, or Methods section).

n/a Confirmed

- ☐ ☒ The exact sample size (n) for each experimental group/condition, given as a discrete number and unit of measurement
- ☐ ☒ An indication of whether measurements were taken from distinct samples or whether the same sample was measured repeatedly
- ☐ ☒ The statistical test(s) used AND whether they are one- or two-sided
Only common tests should be described solely by name; describe more complex techniques in the Methods section.
- ☐ ☒ A description of all covariates tested
- ☐ ☒ A description of any assumptions or corrections, such as tests of normality and adjustment for multiple comparisons
- ☐ ☒ A full description of the statistics including central tendency (e.g. means) or other basic estimates (e.g. regression coefficient) AND variation (e.g. standard deviation) or associated estimates of uncertainty (e.g. confidence intervals)
- ☐ ☒ For null hypothesis testing, the test statistic (e.g. F , t , r) with confidence intervals, effect sizes, degrees of freedom and P value noted
Give P values as exact values whenever suitable.
- ☐ ☒ For Bayesian analysis, information on the choice of priors and Markov chain Monte Carlo settings
- ☒ ☐ For hierarchical and complex designs, identification of the appropriate level for tests and full reporting of outcomes
- ☐ ☒ Estimates of effect sizes (e.g. Cohen's d , Pearson's r), indicating how they were calculated
- ☐ ☒ Clearly defined error bars
State explicitly what error bars represent (e.g. SD, SE, CI)

Our web collection on [statistics for biologists](#) may be useful.

Software and code

Policy information about [availability of computer code](#)

Data collection

Provide a description of all commercial, open source and custom code used to collect the data in this study, specifying the version used OR state that no software was used.

Data analysis

R v3.3.1, BOLT-LMM v2.3, LDSC, GCTA, Locuszoom, PLINK, ANNOVAR

For manuscripts utilizing custom algorithms or software that are central to the research but not yet described in published literature, software must be made available to editors/reviewers upon request. We strongly encourage code deposition in a community repository (e.g. GitHub). See the Nature Research [guidelines for submitting code & software](#) for further information.

Data

Policy information about [availability of data](#)

All manuscripts must include a [data availability statement](#). This statement should provide the following information, where applicable:

- Accession codes, unique identifiers, or web links for publicly available datasets
- A list of figures that have associated raw data
- A description of any restrictions on data availability

SpiroMeta GWAS summary statistics and UK Biobank GWAS summary statistics are available online via LD-Hub (<http://ldsc.broadinstitute.org/ldhub/>). Single-variant

Field-specific reporting

Please select the best fit for your research. If you are not sure, read the appropriate sections before making your selection.

☒ Life sciences ☐ Behavioural & social sciences ☐ Ecological, evolutionary & environmental sciences

For a reference copy of the document with all sections, see [nature.com/authors/policies/ReportingSummary-flat.pdf](https://www.nature.com/authors/policies/ReportingSummary-flat.pdf)

Life sciences study design

All studies must disclose on these points even when the disclosure is negative.

Sample size	In order to maximise power, we used all samples available in UK Biobank and SpiroMeta with good measures of lung function and that had been genotyped giving a total sample size of 400,102.
Data exclusions	For UK Biobank, we excluded samples with low-quality lung function measurements or samples that failed genotyping quality control. Discovery analyses were restricted to those of European ancestry (additional risk score analyses were undertaken in individuals of non-European ancestry with the same exclusion criteria). For SpiroMeta, exclusion criteria for each of the 22 contributing cohorts is described in the supplementary information but are similar to the exclusions for UK Biobank (i.e. genotyping and spirometry quality, and ancestry).
Replication	We only report results that were significantly associated independently in both UK Biobank and SpiroMeta.
Randomization	Not applicable.
Blinding	Blinding was not necessary as the analysts were not involved in the measurement of lung function or genotypes and all samples are anonymised.

Reporting for specific materials, systems and methods

Materials & experimental systems

n/a	Involved in the study
<input checked="" type="checkbox"/>	<input type="checkbox"/> Unique biological materials
<input checked="" type="checkbox"/>	<input type="checkbox"/> Antibodies
<input checked="" type="checkbox"/>	<input type="checkbox"/> Eukaryotic cell lines
<input checked="" type="checkbox"/>	<input type="checkbox"/> Palaeontology
<input checked="" type="checkbox"/>	<input type="checkbox"/> Animals and other organisms
<input type="checkbox"/>	<input checked="" type="checkbox"/> Human research participants

Methods

n/a	Involved in the study
<input checked="" type="checkbox"/>	<input type="checkbox"/> ChIP-seq
<input checked="" type="checkbox"/>	<input type="checkbox"/> Flow cytometry
<input checked="" type="checkbox"/>	<input type="checkbox"/> MRI-based neuroimaging

Human research participants

Policy information about [studies involving human research participants](#)

Population characteristics	UK Biobank is a general population cohort comprising 500,000 individuals age 40-69. The SpiroMeta consortium is comprised of 22 cohorts.
Recruitment	UK Biobank recruitment is described here: http://www.ukbiobank.ac.uk/ . The SpiroMeta cohorts are all population-based, family-based and/or birth cohorts - full details of each cohort are described in the Supplementary information.